Impact of the representation of marine stratocumulus clouds on the anthropogenic aerosol effect

D. Neubauer[1], U. Lohmann[1], C. Hoose[2] and M. G. Frontoso[1,3,*]

[1]{ETH Zurich, Institute for Atmospheric and Climate Science, Switzerland}

[2]{Karlsruhe Institute of Technology, Institute for Meteorology and Climate Research, Germany}

[3]{ETH Zurich, Center for Climate System Modeling, Switzerland}

[*]{now at: RMS, Switzerland}

Correspondence to: D. Neubauer (david.neubauer@env.ethz.ch)

Abstract

Stratocumulus clouds are important for climate by reflecting large amounts of solar radiation back to space. However they are difficult to simulate in global climate models because they form under a sharp inversion and are thin. A comparison of model simulations with the ECHAM6-HAM2 global aerosol climate model to observations, reanalysis and literature data revealed too strong turbulent mixing at the top of stratocumulus clouds and a lack of vertical resolution. Further reasons for cloud biases in stratocumulus regions are the too ‘active’ shallow convection scheme, the cloud cover scheme and possibly too low subsidence rates.

To address some of these issues and improve the representation of stratocumulus clouds we made three distinct changes to ECHAM6-HAM2. With a ‘sharp’ stability function in the turbulent mixing scheme we have observed, similar to previous studies, increases in stratocumulus cloud cover and liquid water path. With an increased vertical resolution in the lower troposphere in ECHAM6-HAM2 the stratocumulus clouds form higher up in the atmosphere and their vertical extent agrees better with reanalysis data. The recently implemented in-cloud aerosol processing in stratiform clouds is used to improve the aerosol representation in the model.

Including the improvements also affects the anthropogenic aerosol effect. In-cloud aerosol processing in ECHAM6-HAM2 leads in the global, annual mean to a decrease of the anthropogenic aerosol effect from -1.19 W/m^2 in the reference simulation to -1.08 W/m^2 while using a 'sharp' stability function leads to an increase to -1.34 W/m^2. The results from the simulations with increased vertical resolution are diverse but increase the anthropogenic aerosol effect to -2.08 W/m^2 at 47 levels and -2.30 W/m^2 at 95 levels.

1 Introduction

Stratocumulus clouds are important for future climate predictions as they have a strong cooling effect (Bretherthon et al., 2004; Williams and Webb, 2009). In a global climate model it is challenging to model stratocumulus clouds because of their small vertical extent. The feedback of low clouds is believed to be a major cause for the model discrepancy in the 2x CO_2 climate sensitivity (Bony and Dufresne, 2005; Stephens, 2005; Williams and Webb, 2009).

It is also challenging to represent the complex interaction between aerosol and clouds in a global climate model. Recent high resolution large eddy simulations (LES) studies showed that the liquid water path may either increase or decrease with increased cloud droplet number concentrations (N_d) in contrast to the thickening from reduced precipitation efficiency (Ackerman et al., 2004; Bretherton et al., 2007; Hill et al., 2008; Sandu et al., 2008; Ackerman et al., 2009; Petters et al., 2013). The thinning is due to increased entrainment of dry free atmospheric air that is associated with increased N_d (Ackerman et al., 2009; Petters et al, 2013). The drying of the boundary layer occurs when the free atmosphere is dry (Ackerman et al., 2004). The increased entrainment is explained either by increased evaporative cooling at cloud top due to stronger turbulence (Ackerman et al., 2004; Hill et al., 2008; Ackerman et al., 2009) or a stronger evaporative cooling efficiency (Bretherton, 2007). The increase in entrainment is substantially reduced when cloud water sedimentation is included in the simulation (Bretherthon et al, 2007; Ackerman et al, 2009). Global climate models typically only represent the reduced precipitation efficiency via an autoconversion parameterisation of cloud water (depending also N_d) to precipitation but no parameterisation of the other interactions.

Typical biases of global climate models and numerical weather prediction models when simulating stratocumulus clouds are a too low cloud amount, a too shallow planetary boundary layer and an underestimation of the liquid water path (Hannay et al., 2009, Medeiros and Stevens, 2011). The diversity that exists among models in simulating stratocumulus clouds increases the uncertainty of the influence of aerosol particles on climate. In an intercomparison study by Stier et al. (2013) the uncertainty in the direct aerosol forcing due to the differences in simulated cloud albedo and used surface albedo among the participating models was assessed. Stratocumulus cloud regions were identified to be among the regions responsible for the largest host model uncertainty in the direct aerosol effect and can therefore be expected to be important for the total anthropogenic aerosol effect.

For the first indirect aerosol effect (cloud albedo effect), Carslaw et al. (2013) systematically evaluated the sources of uncertainty for the simulation of aerosol. Uncertainties in natural emissions cause most uncertainty in cloud radiative forcing, followed by uncertainties in anthropogenic emissions and aerosol processes. Stratocumulus regions were identified as regions with a strong cloud albedo effect and large model uncertainty. Surface albedo and cloud optical depth fields from International Satellite Cloud Climatology Project (ISCCP; Rossow and Schiffer, 1999) D2 data for low level stratiform clouds was used in their study. To evaluate the uncertainty stemming from the simulation of clouds Carslaw et al. (2013) did extra simulations with the 1983–2008 multi-annual ISCCP cloud climatology but found that the sensitivity to the cloud climatology was very small.

As stratocumulus regions are areas of a strong anthropogenic aerosol effect, simulations of the anthropogenic aerosol effect can be expected to depend on the representation of stratocumulus clouds. In our study we investigate the total anthropogenic aerosol effect (also referred to as the effective radiative forcing due to aerosol-cloud and aerosol-radiation interactions, Boucher et al., 2013), including the direct, semi-direct, indirect aerosol effects (cloud albedo, cloud lifetime) as well as effects on mixed-phase, ice and but not convective clouds.

A number of physical processes have to be accounted for when modeling stratocumulus clouds including cloud top radiative cooling which drives turbulent fluxes in the planetary boundary layer, absorption of shortwave fluxes in the cloud layer, entrainment of warm, dry air from the free atmosphere and microphysical processes. The representation of several of these processes are addressed in the general circulation model ECHAM6 (Stevens et al., 2013) coupled to the aerosol module HAM2 (Zhang et al., 2012) and a two-moment cloud microphysics scheme (Lohmann et al., 2007) in this study.

Section 2 summarizes the methodology to evaluate stratocumulus clouds in a global climate model and observational data used. Section 3 gives a description of the model and experiments conducted, the results from which are presented in Sect. 4. The discussion of the results and conclusions follow in Sect. 5.

2 Methodology and observational data

The focus of this study lies on the representation of marine stratocumulus clouds. The analysis of the experiments is therefore confined to stratocumulus regions (and global values where appropriate). Two approaches have been used in recent years for analysis in different cloud regimes. The first one is based on cloud characteristics where a statistical cluster analysis method is used to identify cloud clusters in joint-histograms of cloud optical depth and cloud top pressure (Jakob and Tselioudis, 2003; Gordon et al., 2005; Williams and Tselioudis, 2007; Zhang, 2007; Williams and Webb, 2009; Tsushima et al., 2013). The second approach is based on dynamic and/or thermodynamic regimes (Tselioudis et al., 2000; Norris and Weaver, 2001; Tselioudis and Jakob, 2002; Bony et al., 2004; Williams et al., 2006; Medeiros and Stevens, 2011). We have used the latter approach as it is straight-forward to apply to a global climate model and provides information for the frequency of occurrence of environmental conditions favorable for stratocumulus clouds. This definition of the stratocumulus regime allows, to the extent possible in a global climate model simulation, to separate dynamical (large-scale environment) and other influences on the simulation of stratocumulus clouds.

We define the stratocumulus regime by:

500 hPa vertical velocity > 10 hPa day^{-1} (1)

and to separate trade-wind cumuli from stratocumulus:

lower tropospheric stability (LTS= $\theta_{700hPa} - \theta_{1000hPa}$) > 18.55 K (2)

(θ is the potential temperature), following Medeiros and Stevens (2011). Another criterion for the vertical velocity closer to the inversion height e.g. 700 hPa could be used but we found that this makes little difference for defining the stratocumulus regime in ECHAM6-HAM2. Because of the known issues of satellite observations at high zenith angles and over bright surfaces (see e.g. Zygmuntowska et al., 2012) stratocumulus clouds at high latitudes (> 60°N and > 60°S) have been excluded in this analysis. We also exclude all land areas as we focus on marine stratocumulus clouds. Monthly mean values of potential temperature and vertical velocity were used to compute the stratocumulus regime.

For model evaluation we use satellite data and ERA-Interim reanalysis data (Dee et al., 2011). To take into account limitations in satellite observations (e.g. detection thresholds), different definitions of model variables vs. variables in satellite retrievals and different scales of model grids vs. satellite pixels we use the Cloud-Aersol Lidar and Infrared Pathfinder Satellite Observations (CALIPSO; Winker et al., 2010) simulator from the Cloud Feedback Model Intercomparison Project (CFMIP) Observation Simulator Package (COSP; Bodas-Salcedo et al., 2011). This simulator also separates cloud cover into high, mid and low cloud fractions according to the International Satellite Cloud Climatology Project (ISCCP; Rossow and Schiffer, 1999) definition.

CFMIP also provides satellite data products for the evaluation of climate and weather prediction models (CFMIP-OBS; http://climserv.ipsl.polytechnique.fr/cfmip-obs/). We used the CFMIP-OBS ISCCP, CALIPSO-GOCCP (Chepfer et al., 2010) and Clouds and Earth's Radiant Energy System (CERES) data products. The CFMIP-OBS ISCCP data product is derived from ISCCP (Rossow and Schiffer, 1999) D1 data. Only daytime observations are used and averaged over one month. We extended the CFMIP-OBS ISCCP data product (available for July 1983 to June 2008) using D1 data to cover the time period January 2006 to December 2009 but found no significant differences between the extended period and the time period January 2006 to June 2008 of the original CFMIP-OBS ISCCP data product. From the cloud top pressure/optical thickness histograms we derived high, mid and low cloud cover by integrating the cloud fraction over the optical thickness at each pressure level. The CFMIP-OBS CALIPSO data product we used covers the time period June 2006 to December 2010. The CERES-Energy Balanced and Filled (EBAF; Loeb et al, 2009) data product covers the time period March 2000 to October 2005.

The total anthropogenic aerosol effect (AAE) is calculated using effective radiative forcing (also called the radiative flux perturbation method) that takes fast feedbacks and interactions into account (cloud lifetime effect, semi-direct effect or aerosol interactions with mixed-phase and ice clouds). Effective radiative forcing is computed as the difference in the top of the atmosphere radiation budget between simulations with and without anthropogenic aerosol emissions using the same sea surface temperatures (Hansen et al., 2005; Haywood et al., 2009; Lohmann et al., 2010; Boucher et al., 2013):

$$AAE = \Delta F_{all} = F_{all,PD} - F_{all,PI} \, , \qquad (3)$$

where Δ represents the difference between present-day and pre-industrial aerosol emissions and F_{all} is the all-sky net radiation flux at the top of the atmosphere. AAE is evaluated globally and in the stratocumulus regime. Results for this are presented in Sect. 4.3. The computation of AAE in the stratocumulus regime is described in the following paragraph.

On the one hand using only grid boxes in the analysis where the environmental conditions are suitable for stratocumulus clouds provides additional information and allows to focus on one cloud regime. Where and when the stratocumulus conditions occur depends on the temporal evolution of the modelled atmospheric conditions (see Appendix A). Such a conditional sampling is therefore on the other hand a source of internal variability when comparing different simulations. Global differences by changes in the model physics or resolution or the global anthropogenic aerosol effect are typically much larger than internal variability. In the stratocumulus regime however due to the conditional sampling internal variability can become as large as changes in variables due to model changes or the anthropogenic aerosol effect. Furthermore differences in the stratocumulus regime between simulations cannot be computed as a difference of each grid box at each month as it is typically done for global differences. Due to the conditional sampling an averaging step is necessary before two simulations can be compared. Therefore the statistical significance of model changes or the anthropogenic aerosol effect in the stratocumulus regime is highly relevant. Statistical significance is assessed by applying an unpaired two tails t-test with unequal variances to yearly mean values over all or specific stratocumulus regions of two simulations which are compared. The differences in a variable between two simulations are considered statistically significant if the p-value < 0.1 (i.e. the probability that there are no “real” differences in the variable between the simulations and that observed differences are only due to natural variability is less than 10%, i.e. the null hypothesis is rejected for $p<0.1$). Results of the t-test for variables changes between different experiments and present day and pre-industrial simulations are presented in the Appendix Tables B1 and B2. For differences due to model changes (see Sect. 3, i.e. changes between different experiments) the mean values over the stratocumulus regime are computed as a mean over all grid boxes belonging to the stratocumulus regime at once as the mean values computed this way were found to be statistically significant (or for some variables in the case of including aerosol processing too small to be statistically significant independently of the averaging method). Taking the average over such a large area as the stratocumulus regime can average out differences. Differences in model variables due to anthropogenic aerosol were found to be smaller than the differences between different present-day experiments. We therefore did not average over the whole stratocumulus regime at once but used a different averaging method for the anthropogenic aerosol effect in the stratocumulus regime. We computed yearly mean values in six stratocumulus regions (see Fig. 4) and compared the differences in these six regions between simulations with present day and pre-industrial aerosol emissions and then took a weighted average (Nam and Quaas, 2013 used a similar approach to evaluate boundary layer clouds in satellite and model data).This raises the statistical significance of some model variables globally as the difference in the simulations in some stratocumulus regions can be larger than the internal variability. When computing the spatial average the different size of the grid boxes is taken into account as a weighting factor. The frequency of occurrence of stratocumulus conditions in the six different stratocumulus regions is used as a weighting factor to compute global values from the values in the six regions. This methodology is used for all variables for which differences between present day and pre-industrial simulations are computed e.g. AAE, the change in liquid water path or cloud cover.

3 Model and experiment description

3.1 Model

The general circulation model ECHAM6 (Stevens et al., 2013) coupled to the latest version of the aerosol module HAM2 (Zhang et al., 2012) is used in this study. It includes a two-moment cloud microphysics scheme for cloud droplets and ice crystals where prognostic equations are computed for cloud water, cloud ice, cloud droplet number concentrations and ice crystal number concentrations (Lohmann et al., 2007). The latest version, HAM2.2 includes a size dependent in-cloud scavenging parameterization (Croft et al., 2010) and optionally orographic cirrus clouds (Joos et al., 2010). Hereinafter for the sake of brevity we will refer to it as

HAM2. Aerosol effects on convective clouds are not included. But there is a dependence of cloud droplets detrained from convective clouds on aerosol. The condensate detrained from convective clouds is added to that of the existing stratiform clouds. For liquid clouds the cloud droplet number added from detrainment depends on the number of aerosol particles that can be activated at the convective cloud base.

The impact of aerosols on warm, mixed-phase and ice clouds can be studied using ECHAM6-HAM2. In all experiments we use a fractional cloud cover scheme that diagnoses fractional cloud cover from relative humidity when a critical relative humidity is reached (Sundqvist et al., 1989).

The vertical turbulent diffusion scheme uses a 1.5 order turbulence closure scheme, which includes a simplified prognostic equation for turbulence kinetic energy (TKE) with moist Richardson number (Brinkop and Roeckner, 1995).

We made three distinct changes to ECHAM6-HAM2 for this study:

1) sharp stability function (STAB):

In the TKE scheme used in ECHAM6, the turbulent diffusivities (K_{Turb}) are the product of the turbulent mixing length (l), a stability function (S) and the square root of TKE:

$$K_{Turb} = l * S * \sqrt{TKE} \quad (4)$$

The stability function used in ECHAM6 is a so-called ‘long-tail’ function, which decays slowly with increasing Richardson number (see Fig. 1). We replaced the ‘long-tail’ stability function with a ‘sharp’ stability function (King et al., 2001; Brown et al., 2008; see Fig. 1). As the stability functions differ the most for large Richardson numbers the largest differences in the simulations occur at stable atmospheric conditions. ‘Long-tails’ functions, also used in numerical weather prediction models, are known to result in excessive mixing at high stabilities. This artificial increased mixing was introduced to offset a cold bias in the near-surface temperature and too active synoptic cyclones (see Sandu et al., 2013 and references therein). In the European Centre for Medium-Range Weather Forecasts (ECMWF) numerical weather prediction model the mixing at stable conditions was relaxed in 2007 to avoid the erosion of capping inversions of the planetary boundary layer and thereby dissipation of stratocumulus clouds (Köhler et al., 2011; Holtslag et al., 2013; Sandu et al., 2013). Brown et al. (2008) have found improvements of the operational verification scores in a numerical weather prediction model by changes to the boundary layer scheme that included the use of a 'short-tail' or 'sharp' stability function over the ocean. They also noted that in the Met Office Hadley Centre climate model (HadGEM2; Martin et al., 2011) the 'sharp' stability function cloud be used everywhere (ocean and land). Pithan and Mauritsen (2012) have found an increase in subtropical stratocumulus cloud cover and a decrease in trade wind cumulus when using ECHAM6 with a 'sharp' function. No near-surface temperature cold bias was apparent with the 'sharp' stability function (Pithan, 2013, personal communication). In a recent study Possner et al. (2014) have shown that reducing the mixing at high stability (by reducing the limit for the prescribed minimum eddy diffusivity in their model) improves the simulation of inversions in the regional climate and weather prediction model COSMO.

2) increased vertical resolution (VRES)

The low vertical resolution used in global climate models (GCMs) results in numerical artifacts such as numerical entrainment (Lendering and Holtslag, 2000) and spurious radiative-dynamical interactions at the cloud top interface of stratocumulus clouds (Stevens et al., 1999). We therefore increase the vertical resolution in the lower troposphere in ECHAM6-HAM2 (see Fig. 2). Grenier and Bretherton (2001) have shown that a 1.5 order turbulence closure model can provide good simulations of dry convective boundary layers. With 15 hPa vertical resolution also in stratocumulus-capped boundary layers mixing was simulated properly. The performance of the model simulations of Grenier and Bretherton (2001), especially at coarser resolution, were depending on further details of the model like the implementation of the entrainment closure and the vertical advection scheme. In the current study we use two new vertical grids: L47bl and L95bl. In both grids the new layers are inserted primarily in the boundary layer/lower atmosphere.

To avoid numerical instabilities the time step needs to be increased at higher vertical resolution. From the standard 31 vertical levels (L31) to L47bl the vertical resolution is approximately doubled and the time step is reduced from 720 s to 300 s. With L95bl the vertical resolution is approximately doubled again compared to L47bl or quadruplicated compared to L31 and the time step is reduced to 180 s. The effect of reducing the time step alone is presented in Sect. 4.2.2.

3) Aerosol processing (AP):

Aerosol processing in stratiform clouds by uptake into cloud particles, collision-coalescence, chemical processing inside the cloud particles and release back into the atmosphere changes the aerosol concentration, size distribution, chemical composition and mixing state. By modeling aerosol processing the representation of the mixing state and the size distribution of particles released by evaporation of clouds and precipitation is more realistic. These changes in the aerosol can influence cloud droplet and ice crystal number concentrations and subsequently cloud liquid and ice water paths as well as cloud lifetime and cloud radiative forcing.

HAM2 uses seven modes to describe the total aerosol. We adapted the scheme from Hoose et al. (2008a,b) to ECHAM6-HAM2, to extend the seven modes by an explicit representation of aerosol particles in cloud droplets and ice crystals in stratiform clouds, which are each represented by 5 tracers for sulfate (SO_4), black carbon (BC), organic carbon (OC), sea salt (SS) and mineral dust (DU). Aerosol mass transfers by nucleation and impact scavenging, freezing and evaporation of cloud droplets and melting and sublimation of ice crystals are treated explicitly (see Fig. 3). Aerosol particles from evaporating precipitation are released to modes, which correspond to their size.

3.2 Experiments

The simulations, summarized in Table 1, were conducted with sea surface temperatures and sea ice cover fixed to observed values (AMIP simulations) at T63 (1.9° x 1.9°) spectral resolution using 31 vertical levels (L31) except for the simulations using the new vertical grids. The length of the simulations was 5 years (2006-2010) for L31 after 3 months spin-up. Due to the increased computational demand of the higher vertical resolution the VRES simulations were run only for 1 year (+3 months spin-up). Present day (year 2000) greenhouse gas concentrations were used in all simulations. Each experiment is a pair of runs with present day (year 2000) and pre-industrial (year 1850) aerosol emissions from the AeroCom Phase II dataset (ACCMIP by Angelika Heil, Martin Schultz and colleagues, see http://aerocom.met.no/emissions.html; Lamarque et al., 2010). For the evaluation of stratocumulus clouds in the reference experiment and the experiments for the changes above (Sects. 4.1 and 4.2) present day aerosol emissions have been used. For the evaluation of the anthropogenic aerosol effect the experiments were repeated (5 years after 3 months spin-up) with climatological values for sea surface temperatures and sea ice cover (CLIM simulations; the climatological values are an average for each calendar month of the years 1979-2008) to decrease the natural variability in the experiments (see also Sect. 2).

In addition to the standard experiments a sensitivity simulation with the reference configuration was performed where the precipitation in stratocumulus regions was turned off and another simulation where the parameterization for shallow convective clouds was turned off. Both simulations were run with climatological sea surface temperatures and sea ice cover for one year with present day greenhouse gas and aerosol emissions.

The changes described in Sect. 3.1 lead to an imbalance of the radiative fluxes on top of the atmosphere. The model was therefore re-tuned for the different experiments. Most parameters are kept to the values of the reference simulation and changes are kept to a minimum. Although this may result in being not the optimal parameter settings to be used, the comparison between the different experiments is facilitated. In most experiments only the tuning parameter for the autoconversion rate (ccraut) is changed (see Table 1), which by itself has a small effect on *AAE* (Lohmann and Ferrachat 2010). Lohmann and Ferrachat (2010) varied ccraut values between 1 and 10, in this study ccraut between 3.5 and 12 are used (see Table 1). In this study the same autoconversion parameterization (Khairoutdinov and Kogan 2000) as in Lohmann and Ferrachat (2010) is used. The tuning of the experiments with the new vertical grids L47bl and L95bl is described in more detail in Sect. 4.2.2.

4 Results

4.1 Stratocumulus clouds in reference simulation

The stratocumulus conditions (see Sect. 2) are met in ECHAM6-HAM2 in similar areas as in ERA-Interim but less frequently (Fig. 4). This is because large values of LTS occur 12% less often in ECHAM6-HAM2 than in the reanalysis data (the same is true for other GCMs, see Medeiros and Stevens, 2011) in areas where both stratocumulus conditions are met. Note that with the frequency of occurrence of stratocumulus conditions the simulation of the large-scale environment can be investigated separately from other factors controlling stratocumulus cloud formation which are discussed below. The criterion for subsidence is met 9% less often in ECHAM6-HAM2 than in ERA-INTERIM in these areas. As the conditions of strong LTS and subsidence together are less frequently met in ECHAM6-HAM2, stratocumulus clouds form less often than in ERA-Interim. The stratocumulus regime covers 4.8% of the global area in the reanalysis data, 4.4% in REF, 4.2% in STAB, 3.0% in VRES47 3.0% in VRES95 and 4.5% in AP. Gettelman et al. (2012) altered the stability threshold to adjust the area covered by the stratocumulus regime in their simulations to the same area fraction as in the reanalysis data but found that the results did not change. Due to the smaller area (compared to reanalysis) covered by the stratocumulus regime in our simulations cloud properties like cloud cover, liquid water path or cloud radiative effect will therefore be too low compared to observations. The regime based analysis allows to investigate cloud properties only when the environmental conditions for stratocumulus clouds are met (see Sect. 2. and Appendix A) and therefore to separate between in-regime uncertainties (all influences on stratocumulus clouds formation excluding large-scale dynamical factors) and total uncertainties (in-regime plus frequency of occurrence uncertainty; all influences on stratocumulus clouds formation including dynamical factors). We therefore differentiate in the following between cloud properties in stratocumulus areas (total uncertainty) and stratocumulus regime cloud properties (in-regime uncertainty). As values in the stratocumulus areas include the average frequency of occurrence (≤1) of stratocumulus in a model grid they are typically smaller than values in the stratocumulus regime.

In Fig. 5 a clear underestimation of low level cloud fraction (LCC) in stratocumulus cloud regions in the reference simulation compared to CALIPSO/ISCCP satellite data is visible. When looking only at in-(stratocumulus)regime values, i.e. similar large-scale environmental conditions, the underestimation is less severe: on average 48 % of the stratocumulus regions are cloud covered in the reference simulation compared to 65 % in CALIPSO data. The low cloud cover is significantly lower in ISCCP compared to CALIPSO, whereas it is vice versa for mid cloud cover indicating a problem with the cloud top height in stratocumulus regions in the ISCCP data.

Similar to the cloud fraction also the liquid water path (LWP) is too low in the reference simulation as compared to observations in stratocumulus areas (see Fig. 6). ERA-Interim reanalysis data agrees fairly well with Moderate Resolution Imaging Spectroradiometer (MODIS; MYD08_D3 daily mean level 3 cloud product; King et al., 2003) data and the LWP climatology of the University of Wisconsin (UWisc; O'Dell et al., 2008) derived from satellite-based passive microwave observations (1988-2005) over oceans. On the other hand when looking only at the LWP in the stratocumulus regime, the (in-regime) values for LWP are higher in the reference simulation than in ERA-Interim. The apparent underestimation of LWP is therefore due to the less frequent simulation of large LTS and subsidence in ECHAM6-HAM2.

The shortwave and longwave cloud radiative effects (SWCRE/LWCRE) are too low (see Fig. 7) in the ECHAM6-HAM2 reference simulation compared to CERES data (Loeb et al., 2009). The in-regime value for the shortwave cloud radiative effect of the simulation agrees quite well with the observational data. The LWCRE on the other hand is underestimated also when only grid points that meet stratocumulus conditions are considered. This is not associated with stratocumulus clouds but due to a lack of mid-level and high clouds in stratocumulus regions in the reference simulation. The net cloud radiative effect is therefore too negative in stratocumulus regions in ECHAM6-HAM2.

In Fig. 8 vertical profiles of relative humidity, potential temperature, cloud cover and liquid water content in stratocumulus regions for the reference simulation and ERA-Interim are shown. The inversion in temperature and humidity is not represented well in the reference simulation, which is due mostly to the coarse resolution used in the reference simulation.

The cloud cover and liquid water content profiles show that stratocumulus clouds form too low in the atmosphere and are too shallow in ECHAM6-HAM2. The liquid water content is too high resulting in the observed overestimation of LWP.

The mean diurnal cycle of liquid water path (LWP) in all stratocumulus regions from one month of a ECHAM6-HAM2 simulation is displayed in Fig. 9. Also shown is the diurnal cycle in different regions from Wood et al. (2002) who examined two years of TMI (Tropical Rainfall Measuring Mission Microwave Imager) satellite microwave radiometer data. Wood et al. (2002) found that the diurnal cycle was more pronounced in the SE Pacific and in the SE Atlantic. We therefore chose for a comparison the month of October (2006) when in the SE Pacific and in the SE Atlantic the stratocumulus cloud cover is large (because of the large amount of data involved we were not able to compute the output for longer time periods). The mean LWP is lower in this particular month as the multiyear average (see Fig. 6). The difference in the morning maximum and the afternoon minimum of LWP, normalized to the mean LWP, in ECHAM6-HAM2 (26%) agrees quite well with the TMI data (20-28%, depending on the region).

To summarize, ECHAM6-HAM2 has cloud biases in stratocumulus cloud regions that are typical for GCMs: the cloud form too low and are too shallow, low cloud cover, liquid water path and the shortwave cloud radiative effect are underestimated. When looking only at data points where the environmental conditions are favorable for stratocumulus clouds (in-regime values) these biases are reduced. The monthly average diurnal cycle of stratocumulus clouds simulated with ECHAM6-HAM2 agrees well with observations.

4.2 Changes for stratocumulus clouds

4.2.1 Reduced turbulent mixing in stable conditions (STAB)

In Fig. 10 changes in cloud properties are shown when the long-tails stability function of ECHAM6-HAM2 is replaced by a ‘sharp’ stability function. Both the cloud cover and the liquid water path increase in the stratocumulus regime whereas in other regions the changes are small. The in-regime low cloud cover increases by 5.3% and the LWP increases by 8.2 g/m^2. This leads to a more negative SWCRE by -2.5 W/m^2. The frequency of occurrence of stratocumulus regions is too low in the STAB experiments compared to reanalysis data and even lower than in the REF experiment (Fig. 4). The global changes in cloud properties by using a ‘sharp’ stability function are rather patchy. In some regions there is an increase in cloud cover and LWP, whereas in other regions there is a decrease. On average these changes almost cancel each other and the averaged change in total cloud cover and liquid water path between the simulation with a ‘sharp’ stability function and the reference simulation is small.

The vertical cloud properties shown in Fig. 8 in the stratocumulus regime reveal subtle changes by using a ‘sharp’ stability function. While stratocumulus clouds still form too low and their vertical extension seems to be limited, cloud cover and liquid water content are reduced above the inversion and reduced below as would be expected by a reduction of mixing at cloud top.

Two one year simulations with climatological sea surface temperatures and sea ice cover and otherwise the same setup as REF and STAB were conducted to diagnose vertical profiles of the turbulent diffusion coefficients (K_m,K_h), turbulent kinetic energy (TKE) and the stability function in the stratocumulus regime. The results are shown in Fig. 11 and indeed the stability function is decreased above the inversion with the 'sharp' stability function. The turbulent kinetic energy (TKE) increases slightly in the cloud layer with the 'sharp' stability function and decreases above. Due to the coarse vertical resolution TKE is produced in the cloud layer rather than at its top.

4.2.2 Increased vertical resolution (VRES47, VRES95, VRES47+STAB)

An increase of the vertical resolution leads to a degradation of the simulations as parameters used in the parameterization of sub grid processes may depend on the resolution. In a sensitivity simulation an autoconversion rate parameter (ccraut) of 12 was necessary to achieve a balance of radiative fluxes at the top of the atmosphere. This large autoconversion rate leads to more precipitation in the stratocumulus regime as well as strong reductions in cloud cover and liquid water path. For the experiments with increased vertical resolution we used therefore tuning parameters, when possible, which showed no strong effect on stratocumulus clouds cloud cover in sensitivity simulations. For L47bl ccraut was kept as in the reference simulation and a parameter for the entrainment rate of deep convection was adjusted instead (entrpen=$1.5\cdot10^{-4}$ instead of entrpen=$3.5\cdot10^{-4}$ in the reference simulation). For L95bl ccraut=12 was necessary in addition to the adjustment in the entrainment rate of deep convection (entrpen=$1\cdot10^{-4}$) to achieve radiation balance. Mean zonal winds, surface pressure and ocean surface stress are very similar to reanalysis data and the reference simulation in the VRES experiments. For L95bl the zonal winds are weaker in the Pacific storm-tracks but this small difference should not affect stratocumulus regions.

To estimate the effect of the reduction of the time step the present day reference simulation (L31) was repeated with reduced time steps of 300 s and 180 s. This leads to significant increases in condensation and deposition rates at shorter time steps and reduced vertical velocities due to reduced turbulent kinetic energy (TKE). This time step dependence will be fixed in newer versions of the ECHAM6 GCM (ECHAM6.2 onwards; Mauritsen T., pers. comm.), but unfortunately they are not yet coupled to the aerosol scheme. The reduced TKE leads to a reduced vertical velocity, which then favors depositional growth of ice crystals at the expense of condensational growth of cloud droplets (Wegener-Bergeron-Findeisen process). In stratocumulus regions the reduced TKE reduces the cloud cover significantly when the time step is reduced. The reduction in cloud cover in the stratocumulus regime in the VRES experiments can therefore be attributed to the reduction of the time step and the subsequent reduction of TKE. The changes in condensation/deposition/TKE also lead to changes in convection. Mid-level convection in the storm tracks is replaced by shallow convection. In the tropics and subtropics shallow convection is replaced by deep and mid-level convection. These changes in convection correlate with changes in AAE. AAE increases from -1.19 W/m^2 @ 720 s to -1.50 W/m^2 @ 300 s and to -1.33 W/m^2 @ 180 s. Changes in the aerosol are small when the time step is reduced and they do not correspond to the changes in AAE. The only exception are strong decreases in dust emissions by -35% (720 s – 300 s) and -37% (720 s – 180 s) but this also do not seem to affect AAE. The dust emissions are very sensitive to changes in wind velocities (and to lesser extent to soil moisture) and the threshold friction velocity may have to be adjusted to a different model setup.

The different tuning and the reduced time steps are necessary for increasing the vertical resolution. The effects of changing the vertical resolution described below are not entirely due to the change in the vertical resolution alone but also to these necessary changes in the model setup.

The increase of the vertical resolution has an ambiguous impact on stratocumulus clouds. Figure 12 shows that with L47bl the already small low cloud cover and the LWP in the stratocumulus regime decrease and the net cloud radiative effect is less negative compared to L31 in the reference simulation. The smaller low clouds cover in the stratocumulus regime can be explained in part by the decreased TKE due to the smaller time step necessary. By the decrease of the time step in the reference simulation a decrease of 3% in the low cloud cover occurred. The decrease in low clouds is compensated partly by a small increase in mid-level clouds but the total cloud cover decreases with L47bl in the stratocumulus regime (not shown). The cloud cover in regions of shallow convective clouds increases (not shown) and compensates the decrease in the stratocumulus regime whereas other regions show only small changes. The vertical profiles of relative humidity and potential temperature do not change significantly with L47bl in the stratocumulus regime compared to the reference simulation (see Fig. 13). The clouds seem to form higher up in the atmosphere but the cloud cover and the liquid water content are reduced. Around 800 hPa the liquid water content is larger than in the reanalysis data. This is the result of too much vertical transport as the cloud cover in the simulation with L47bl is not significantly larger around 800 hPa as in the reanalysis data. Increasing the vertical resolution further has a somewhat different effect. With the highest vertical resolution grid L95bl used in this study there is an increase in cloud cover and liquid water path in the stratocumulus regime (Fig. 12). The pattern appears like a spatial shift of the clouds but actually there are two changes partly compensating each other. The increase in cloud cover and LWP is in areas where also shallow cumulus clouds may appear (the shallow convection frequency is reduced in the VRES95 experiment see Fig. C1) and not in the 'core' stratocumulus regions, where the same decrease of cloud cover and LWP as in the VRES47 simulation occurs (due in part to reduced turbulent vertical velocity). In VRES95 the vertical cloud properties are improved further i.e. the clouds form higher up in the atmosphere and their vertical extent agrees better with reanalysis data. That there is no clear improvement in ECHAM6-HAM2 when increasing the vertical resolution is in agreement with other studies. Stevens et al. (2007) have shown that LWP and the planetary boundary layer (PBL) depth are underestimated in ERA-40 (Uppala et al. 2005) and ERA-15 (Gibson et al. 1997) although the vertical resolution was increased from ERA-15 to ERA-40. With the Köhler (2005) PBL scheme the representation of stratocumulus clouds was improved in the ECMWF model without increasing the vertical resolution. Although increasing the vertical resolution in single column models often improves the representation of stable/cloudy boundary layers (Grenier and Bretherton, 2001; Zhu et al., 2005; Wyant et al., 2007; Gettelman and Morrison, 2014) the same must not necessarily be true in a global model. Feedbacks between the dynamics and the physical parameterizations can cause differences in the biases of a parameterization in a global model and a single column model (Petch et al., 2007; Zhang et al., 2013).

The vertical profiles of relative humidity and cloud properties improve with the L95bl-resolution and are quite similar to reanalysis data. The clouds are forming higher up in the atmosphere and have a larger vertical extent (see Fig. 13). The higher cloud cover and LWP at higher altitudes in the VRES experiments compared to ERA-Interim and the lower cloud cover and LWP at lower altitudes indicate too much turbulent and convective vertical transport at the cloud top in the VRES experiments. There are still too few stratocumulus clouds even with L95bl in ECHAM6-HAM2 as only the cloud cover in stratocumulus regions increases whereas the frequency of occurrence of those regions is still too low or even lower in the VRES experiments compared to reanalysis data (Fig. 4). The aerosol burden decreases for all aerosol species except sulfate (SO_4) (see Table 2) in the VRES experiments as compared to the reference simulation. Although the emission rates are quite similar the aerosol particles are removed faster from the atmosphere in the VRES experiments due to increased wet deposition rates (cf. Fig. 14). In the VRES95 experiment also the dry deposition rate is increased. One exception is mineral dust (DU) for which the emission is reduced by -36 % in the VRES47 experiment and by -49 % in the VRES experiment. As mentioned above dust emissions are very sensitive to wind velocities. Although the monthly mean 10m wind velocities do not change much between the experiments, shorter fluctuations in the wind velocities could considerably alter the dust emissions.

In the VRES47+STAB experiment the clouds in the stratocumulus regime are even further reduced as in the VRES47 experiment. The low cloud cover is lower by -11.4%, LWP decreases by -9.7 g/m^2 and SWCRE by 11.5 W/m^2 in the stratocumulus regime compared to the REF experiment (not shown). The vertical cloud properties are less similar to reanalysis data in the VRES47+STAB experiment than in the VRES47 experiment (see Figs. 8 and 13). The cloud cover is further reduced around 900 hPa but too high around 800 and 1000 hPa. The vertical profile of liquid water content changes similar to the cloud cover when the ‘sharp’ stability function is used together with the L47bl vertical grid. The liquid water content is reduced around 900 hPa but larger close to the surface in the VRES47+STAB experiment than in VRES47. Around 800 hPa the liquid water content in the VRES47+STAB and VRES47 experiments is too large compared to reanalysis, irrespective of the stability function used. This indicates that not only turbulent but also convective transport is too large around 800 hPa in the stratocumulus regime.

4.2.3 Aerosol processing in stratiform clouds (AP, STAB+AP)

The cloud condensation nuclei concentration at 0.1 % supersaturation roughly doubles in the AP experiment compared to the reference simulation in the stratocumulus regime while the cloud droplet number concentration only increases by 13 %. Although the aerosol load, aerosol size distribution and mixing state change when using in-cloud aerosol processing (not shown), this hardly affects cloud properties in stratocumulus cloud regions. In a simulation with aerosol processing the cloud cover is lower by 0.3%, LWP increases by 0.4 g/m^2 and NETCRE by 0.8 W/m^2 in the stratocumulus regime. The frequency of occurrence of stratocumulus regions is similar to the REF experiment (see Fig. 4). Also the vertical profiles of relative humidity, potential temperature, cloud cover and liquid water content in stratocumulus regions are similar to the reference simulation. In-cloud aerosol processing seems to alter only the aerosol in stratocumulus regions not the clouds.

In the experiment STAB+AP where the 'sharp' stability function and aerosol processing are used together the stratocumulus clouds are very similar to the STAB experiment. The low cloud cover is higher by 4.8%, LWP increases by 15.5 g/m^2 and SWCRE by -4.4 W/m^2 in the stratocumulus regime compared to the REF experiment (not shown). Turbulent mixing at the top of the boundary layer also affects the aerosol. The AOD is slightly lower in the STAB+AP experiment than in the AP experiment.

4.3 Anthropogenic aerosol effect

In Fig. 15 the total anthropogenic aerosol effect (AAE) is shown globally. Stratocumulus regions are regions of a strong negative AAE as are regions close to the industrial centers of the world and biomass burning regions. Table 2 lists aerosol, cloud and forcing parameters for present day CLIM simulations for all experiments. The large SS burden and AOD in the AP experiment are due to too large sea salt emissions (see Hoose et al., 2008a). Table 3 lists AAE and other parameters for all experiments globally and in the stratocumulus regime. The focus of this study lies on the representation of marine stratocumulus clouds. Therefore AAE is computed also in the stratocumulus regime. For the computation of the change in the aerosol effect in the stratocumulus regime (AAE_{Sc}) the stratocumulus conditions have been computed for the present day and pre-industrial aerosol simulations separately. There are differences in the appearance of these conditions in both space and time between present day and pre-industrial aerosol simulations due to internal variability. This variability can be comparable to the anthropogenic aerosol effect. Regionally averaged values for the stratocumulus regime were therefore computed (see Sect. 2; Table 3).

Figure 16 shows the change in AAE between the reference simulation and simulations with the 'sharp' stability function (STAP), aerosol processing (AP) and increased vertical resolution (VRES47, VRES95) respectively. In the experiment with the 'sharp' stability function the change in LWP between the simulation with present day and pre-industrial aerosol and the change in cloud cover are comparable to the reference experiment (see Table 3). AAE increases globally (-0.25 W/m^2) and in the stratocumulus regime in the STAB experiment. The global increase in AAE is actually due to a stronger decrease of the longwave aerosol forcing than the shortwave aerosol forcing. Aerosol number and mass are reduced by approx. 10% in the stratocumulus regime with the 'sharp' stability function whereas global mean values of aerosol number and mass are similar for the STAB and REF experiments. The reduction in background aerosol load in the stratocumulus regime with the 'sharp' stability function and the accompanied increased susceptibility of AAE_{Sc} to anthropogenic aerosol (Carslaw et al., 2013) as well as the larger changes of LWP_{Sc} and LCC_{Sc} can explain the increase in AAE_{Sc} in the STAB experiment compared to the reference experiment.

There is a reduction in AAE compared to the reference simulation in the experiment with aerosol processing i.e. in regions of a negative AAE in the reference simulation, AAE becomes less negative; in regions of a positive AAE in the reference simulation, AAE becomes less positive and in the global average AAE is less negative. Note that the impact of aerosol processing may be different in high resolution e.g. large eddy simulations of stratocumulus clouds as in our GCM simulation the important 'evaporation-entrainment' feedback (Xue and Feingold, 2006) is not accounted for explicitly. In the AP experiment the background aerosol is increased. This leads to a reduced susceptibility of the clouds to anthropogenic aerosol. The reduction occures everywhere on the globe in the simulation with aerosol processing. Both shortwave and longwave forcings are weaker but on average the forcing becomes less negative (-1.08 W/m^2 compared to -1.19 W/m^2 in the reference simulation globally).

Running the model with the 'sharp' stability function and aerosol processing together (STAB+AP) further amplifies the reduction in AAE. In the stratocumulus regime AAE_{Sc} also seems to decrease in the STAB+AP experiment but the differences between present day and pre-industrial aerosol simulations are too small to be significant compared to internal variability.

In the VRES experiments there is a strong increase in AAE. As discussed in Sect. 4.2.2 there are changes in aerosol emission and removal in the VRES experiments compared to the reference simulation leading to smaller aerosol burdens. These changes seem not to be the direct result of the changed model resolution but of the changes in the clouds. Changes in clouds, as they occur in the VRES experiments, change also the atmospheric aerosol by changing wet deposition or production of SO_4 by wet chemistry. Reduced wet deposition of large aerosol particles would decrease the condensation rate of SO_4 to atmospheric aerosol particles and increase the nucleation rate of SO_4 leading to increased CCN. Also increased production of SO_4 would lead to increased CCN. With these two mechanisms changes in aerosol cloud interactions due to changes in the clouds could be amplified by subsequent changes in aerosol. In Fig. 14 the change in wet deposition of aerosol mass and the change in production of SO_4 by wet chemistry between the VRES95 and the REF experiment are shown. There seems to be a correlation between the increase of wet deposition and the increase of SO_4 production and the stronger AAE in the VRES95 experiment in many regions.

In the VRES47 experiment both shortwave and longwave aerosol forcing increase compared to the REF experiment. The resulting AAE is stronger in VRES47 than in REF. The change in the shortwave and longwave aerosol forcing comes probably from changes in cloud regimes due to the increased vertical resolution and different entrainment rates for deep convection. In the stratocumulus regimes there is a similar strong increase in AAE_{Sc} in the VRES47 experiment as globally.

Combining the increased vertical resolution with the ‘sharp’ stability function (VRES47+STAB) leads to a more negative AAE globally compared to the reference experiment and similar AAE compared to VRES47. This is due to decreased shortwave and longwave aerosol forcing that compensate each other compared to the VRES47 experiment. The shortwave aerosol forcing is smaller in the stratocumulus regime in VRES47+STAB but AAE_{Sc} is quite similar to VRES47 and STAB.

In the VRES95 experiment AAE is strongly increased. This is due to a lower aerosol load in the present day and pre-industrial aerosol simulations at this high vertical resolution and the subsequent increased susceptibility to anthropogenic aerosol. In the stratocumulus regime a similar strong increase compared to REF in AAE_{Sc} is observed.

5 Summary and conclusions

We have performed several simulations to identify cloud biases in the stratocumulus regime and to improve the representation of stratocumulus clouds and the aerosol in the stratocumulus regime. The impact of these changes on the anthropogenic aerosol effect have also been investigated. The biases in ECHAM6-HAM2 are typical for global models: the clouds form too low and are too shallow, low cloud cover, liquid water path and the shortwave cloud radiative effect are underestimated. In the stratocumulus regime (diagnosed by environmental conditions) these biases are reduced.

The formation of stratocumulus clouds depends on many factors. Their representation in large-scale models requires a correct simulation of the large-scale environment. The main reasons for the cloud biases in regions with high stratocumulus cloud cover in ECHAM6-HAM2 as follows:

- Too strong turbulent mixing at stable conditions: At high vertical resolution the vertical cloud properties indicate a too strong mixing at the top of stratocumulus clouds in ECHAM6-HAM2 and too much convective transport. The turbulent mixing at stable conditions can be reduced by using a ‘sharp’ stability function in the TKE scheme of ECHAM6. This improves the stratocumulus cloud cover and liquid water path but changes the vertical cloud properties only modestly. The stratocumulus clouds in ECHAM6-HAM2 at high vertical resolution have a larger vertical extent but their coverage is smaller at lower altitudes than in ERA-Interim. This may be explained by too strong entrainment of warm, dry free tropospheric air into the PBL, which is reduced with the ‘sharp’ stability function, and too much convective transport of moisture to higher levels. The improvement by using a ‘sharp’ stability function is not sufficient to reconcile the simulated low cloud cover with that of satellite observations.

- Too ‘active’ shallow convective scheme: Another reason for the lack of stratocumulus clouds appears to be the over-active shallow convection scheme in ECHAM6-HAM2. Isotta et al. (2011) have shown that the Tiedtke-shallow-convection scheme (Tiedtke, 1989) used in ECHAM5-HAM (Roeckner et al., 2003; Stier et al., 2005; also used in ECHAM6-HAM2) activates too frequently compared to large eddy simulations and observations of the frequency of cumulus clouds. Their transient shallow-convection scheme decreased the frequency of shallow convection which was compensated by increased stratus and stratocumulus (a similar decrease of shallow-convection frequency and increase of LWP in the stratocumulus regime was observed in the VRES95 experiment, see Fig. C1). In a recent study Nam et al. (2014) compared three boundary layer cloud schemes in ECHAM5 to the standard scheme used in ECHAM5 and CALIPSO and CloudSat satellite observations. All three schemes improved low cloud cover and precipitation in the (sub)tropics compared to the standard scheme (note that their ECHAM5_Trig model is similar to what is used in ECHAM6). Two of the new schemes reduced the frequency of shallow convection compared to standard ECHAM5. The third new scheme does not compute shallow convection separately.

  By turning off shallow convection completely in a sensitivity study we found that stratocumulus clouds were forming higher up and were thicker. The improvement is almost as large as by increasing the vertical resolution. Turning off shallow convection also increased the low cloud cover in the stratocumulus regime. Changing the shallow convection scheme in ECHAM6 would probably be beneficial for representing stratocumulus clouds.
- The relative humidity based cloud cover scheme: A sensitivity study where precipitation in the stratocumulus regime was turned off showed an impact mainly on liquid water path, cloud optical properties and cloud radiative effects. LWP and cloud optical depth (COD) approximately double in the stratocumulus regime without precipitation compared to the reference simulation and SWCRE is increased by 21% resulting in a more negative net cloud radiative effect (NETCRE in worse agreement with observations). The low cloud cover increases only by 3% from 47.7% to 50.7 %. This strong increase in LWP by turning off precipitation which hardly affects low cloud cover indicates that the relative humidity based cloud cover scheme used for the simulations produces not enough cloud cover in the stratocumulus regime (see also Fig. 5).

- Lack of vertical resolution: Stratocumulus clouds in ECHAM6-HAM2 form too low and are too shallow. With an increased vertical resolution the clouds are forming higher up and are quite similar to the clouds in the ERA-Interim stratocumulus regime. A simple increase of the vertical resolution (at unchanged horizontal resolution) improves the vertical cloud properties in the stratocumulus regime but affects other parts of the model and leads to a degradation of the simulation. Diagnosing the actual inversion height (cloud top) in stratocumulus regions as in the schemes of Grenier and Bretherton (2001; applied to ECHAM5-HAM in Siegenthaler-Le Drian, 2010) could improve stratocumulus clouds while keeping the interaction with other parts of the model at a minimum.
- Possibly too low subsidence rates: Environmental conditions suitable for stratocumulus clouds appear 8% less frequent in ECHAM6-HAM2 (4.4% of the global area in the REF experiment) as in reanalysis data (4.8%) due to a too low LTS and too low subsidence rates. The underestimation of the frequency of stratocumulus conditions appears in all simulations conducted in this study, in particular also in the simulations with reduced turbulent mixing at the top of the stratocumulus clouds and increased vertical resolution. Subsidence rates are lower in ECHAM6-HAM2 than in ERA-Interim which might explain the lack of inversions.
- The monthly average diurnal cycle of liquid water path of stratocumulus clouds modeled in ECHAM6-HAM2 on the other hand agrees well with observations.

Our simulations indicate that no single measure brings the simulated stratocumulus clouds in ECHAM6-HAM2 in agreement with observations. Changes to three parts of the model will be necessary to further improve the simulation of stratocumulus clouds in ECHAM6-HAM2:

- Changes in the cloud cover scheme,
- Changes in the shallow convection scheme and
- Changes in the boundary layer scheme.

From our simulations with changes in model resolution and physics to better represent clouds and aerosol in the stratocumulus regime we conclude that the anthropogenic aerosol effect (AAE) is sensitive to changes in (stratocumulus) clouds:

Aerosol processing in stratiform clouds has only a small impact on cloud properties in ECHAM6-HAM2 but it reduces the anthropogenic aerosol effect globally from -1.19 W/m^2 in the reference simulation to -1.08 W/m^2. In the simulations performed in this study the cloud droplet number concentration is quite stable in the stratocumulus regime as it increased only by 23 % in the sensitivity study with precipitation turned off in the stratocumulus regime and by only 13 % in the aerosol processing experiment where the cloud condensation nuclei concentration (CCN) approximately doubles.

The ‘sharp’ stability function leads to an increase in AAE of 0.15 W/m^2 to -1.34 W/m^2. In simulations VRES47 and VRES95 AAE strongly increases to -2.08 W/m^2 and -2.30 W/m^2 respectively. AAE in the stratocumulus regime is generally stronger than in the global mean and so are the changes between the different experiments. These sensitivity studies show the importance of a good representation of stratocumulus clouds for simulations of the anthropogenic aerosol effect.

Appendix A: Definitions of terms in the stratocumulus regime

Stratocumulus regime:

The stratocumulus regime is defined by environmental conditions (Eqns. 1, 2). At T63 (1.9° x 1.9°) horizontal resolution (used in this study) the surface of Earth is divided in grid areas. At each point in time, in certain areas of the world this conditions will be met. All such select areas together constitute the stratocumulus regime.

As environmental conditions change over time also the such defined areas change over time. So at each point of time the stratocumulus regime may constitute of different geographical areas. Fig. A1 shows the stratocumulus regime in January and July 2006. The variation that occurs between different months makes it difficult to compare values from a specific month between two simulations. The annual average where the environmental conditions favorable for stratocumulus clouds are met although is quite constant. Furthermore the conditions are often met in specific, geographical areas. Monthly mean values of LTS and vertical velocity were used to compute the stratocumulus regime.

Note that the term stratocumulus regime used in this study refers only to the presence of specific environmental conditions and not necessarily to the presence of clouds. The conditions were chosen to be favorable for stratocumulus clouds but that does not mean that in every area within the stratocumulus regime a cloud must be present.

This definition of the stratocumulus regime allows, to the extent possible in a GCM simulation, to separate dynamical and other influences on the simulation of stratocumulus clouds. Dynamics alter when and where stratocumulus conditions are present but once they are met the properties of stratocumulus clouds in the stratocumulus regime (in-regime values) can be considered to depend mainly on the parameterizations used in the model and not on the (resolved) large-scale dynamics.

Stratocumulus regions:

Fig. 4 shows a 5 year average of the occurrence of the environmental conditions favorable for stratocumulus clouds. It is apparent that in some geographical areas the environmental conditions favorable for stratocumulus clouds are met more than 25% of the time in some areas even more than 50% of the time or even more frequently. We use this to define six, geographically distinct stratocumulus regions by hand (also shown in Fig. 4).

In-regime values/uncertainty:

These are average values of a certain quantity over all areas where the environmental conditions favorable for stratocumulus clouds are met, i.e. average values for the stratocumulus regime. Note that not in every area within the stratocumulus regime a cloud must be present. For example average values of low cloud cover are shown in Fig. 5. In-regime values are shown in many Figures below the panels in this study (marked by the subscript $_{Sc}$) and must not be confused with in cloud values. The in-regime values can be considered to depend not (or at least less) on the large-scale dynamics of the model and are used therefore to identify uncertainty due the turbulent mixing scheme, the convective parameterizations, cloud microphysics etc. but not dynamics (in-regime uncertainty).

Total uncertainty:

The in-regime values can be multiplied by the frequency of occurrence of stratocumulus conditions. These values give then the total uncertainty due to the dynamics of the models and other model parts compared to reanalysis data and observations. In-regime values multiplied by the frequency of occurrence of stratocumulus conditions are displayed in many Figures of the present study to facilitate the assessment of the total model uncertainty.

Appendix B: Statistical significance of results in the stratocumulus regime

Results of the t-test for variables changes between different experiments and present day and pre-industrial simulations are presented in the Tables B1 and B2.

Appendix C: Changes in shallow convection

The frequency of the activation of the shallow-convection scheme in the REF, STAB, VRES47 and VRES95 experiments is shown in Fig. C1.

Acknowledgements

D. Neubauer gratefully acknowledges the support by the Austrian Science Fund (FWF): J 3402-N29 (Erwin Schrödinger Fellowship Abroad) and ETH Zurich. The EU FP7 projects EUCLIPSE (244067) and COMBINE (226520) are acknowledged for financial support. This work was supported by a grant from the Swiss National Supercomputing Centre-CSCS under project ID s431. We would like to thank Bjorn Stevens, Thorsten Mauritsen, Felix Pithan, Sebastian Rast, Andreas Chlond, Erich Roeckner, Andrew Gettelman, Graham Feingold, Colombe Siegenthaler-Le Drian, Anna Possner, Sylvaine Ferrachat, Angela Meyer and Franziska Glaßmeier for discussions and technical help.

Supplementary material is available online.

References

Baker, M. and Charlson, R.: Bistability of CCN concentrations and thermodynamics in the cloud-topped boundary layer, Nature, 345, 142–145, doi: 10.1038/345142a0, 1990.

Bodas-Salcedo, A., Webb, M. J., Bony, S., Chepfer, H., Dufresne, J.-L., Klein, S. A., Zhang, Y., Marchand, R., Haynes, J. M., Pincus, R. and John, V. O.: COSP: Satellite simulation software for model assessment, B. Am. Meteorol. Soc. 92, 1023-1043, doi: 10.1175/2011BAMS2856.1, 2011.

Bony, S., Dufresne, J. L., Le Treut, H., Morcrette, J. J. and Senior, C. A.: On dynamic and thermodynamic components of cloud changes, Clim. Dyn., 22, 71–86, doi:10.1007/s00382-003-0369-6, 2004.

Bony, S. and Dufresne, J. L.: Marine boundary layer clouds at the heart of tropical cloud feedback uncertainties in climate models, Geophys. Res. Lett., 32, L20806, doi: 10.1029/2005GL023851, 2005.

Boucher, O., Randall, D., Artaxo, P., Bretherton, C., Feingold, G., Forster, P., Kerminen, V.-M., Kondo, Y., Liao, H., Lohmann, U., Rasch, P., Satheesh, S.K., Sherwood, S., Stevens, B. and Zhang, X.Y.: Clouds and Aerosols, in: Climate Change 2013: The Physical Science Basis. Contribution of Working Group I to the Fifth Assessment Report of the Intergovernmental Panel on Climate Change [Stocker, T.F., Qin, D., Plattner, G.-K., Tignor, M., Allen, S.K., Boschung, J., Nauels, A., Xia, Y., Bex V., and Midgley, P.M. (eds.)], Cambridge University Press, Cambridge, United Kingdom and New York, NY, USA, 2013.

Bretherton, C. S., Uttal, T., Fairall, C. W., Yuter, S. E., Weller, R. A., Baumgardner, D., Comstock, K., Wood, R. and Raga, G. B.: The Epic 2001 Stratocumuls Study, B. Am. Meteorol. Soc., 85, 967-977, doi: 10.1175/BAMS-85-7-967, 2004.

Brinkop, B. and Roeckner, E.: Sensitivity of a general circulation model to parametrizations of cloud-turbulence interactions in the atmospheric boundary layer, Tellus, 47, 197–220, doi: 10.1034/j.1600-0870.1995.t01-1-00004.x, 1995.

Brown, A. R., Beare, R. J., Edwards, J. M., Lock, A. P., Keogh, S. J., Milton, S. F. and Walters, D. N.: Upgrades to the Boundary-Layer Scheme in the Met Office Numerical Weather Prediction Model, Bound.-Lay. Meteorol., 128, 117-132, doi: 10.1007/s10546-008-9275-0, 2008.

Carslaw, K. S., Lee, L. A., Reddington, C. L., Pringle, K. J., Rap, A., Forster, P. M., Mann, G. W., Spracklen, D. V., Woodhouse, M. T., Regayre, L. A. and Pierce, J. R.: Large contribution of natural aerosols to uncertainty in indirect forcing, Nature, 503, 67-71, doi: 10.1038/nature12674, 2013.

Chepfer, H., Bony, S., Winker, D., Cesana, G., Dufresne, J. L., Minnis, P., Stubenrauch, C. J., and Zeng, S.: The GCM oriented CALIPSO Cloud Product (CALIPSO-GOCCP), J. Geophys. Res., 115, D00H16, doi:10.1029/2009JD012251, 2010.

Croft, B., Lohmann, U., Martin, R. V., Stier, P., Wurzler, S., Feichter, J., Hoose, C., Heikkilä U., van Donkelaar, A. and Ferrachat., S.: Influences of in-cloud aerosol scavenging parameterizations on aerosol concentrations and wet deposition in ECHAM5-HAM, Atmos. Chem. Phys., 10, doi: 10.5194/acp-10-1511-2010, 2010.

Dee, D. P., Uppala, S. M., Simmons, A. J., Berrisford, P., Poli, P., Kobayashi, S., Andrae, U., Balmaseda, M. A., Balsamo, G., Bauer, P., Bechtold, P., Beljaars, A. C. M., van de Berg, L., Bidlot, J., Bormann, N., Delsol, C., Dragani, R., Fuentes, M., Geer, A. J., Haimberger, L., Healy, S. B., Hersbach, H., Hólm, E. V., Isaksen, L., Kallberg, P., Köhler, M., Matricardi, M., McNally, A. P., Monge-Sanz, B. M., Morcrette, J.-J., Park, B.-K., Peubey, C., de Rosnay, P., Tavolato, C., Thépaut, J.-N.and Vitart, F.: The ERA-Interim reanalysis: configuration and performance of the data assimilation system. Q. J. Roy. Meteor. Soc., 137, 553–597, doi: 10.1002/qj.828, 2011.

Gettelman, A. and Morrison, H.: Advanced Two-Moment Bulk Microphysics for Global Models. Part I: Off-Line Tests and Comparison with Other Schemes, 2014, submitted.

Gettelman, A., Kay, J. E. and Shell, K. M.: The Evolution of Climate Sensitivity and Climate Feedbacks in the Community Atmosphere Model, J. Climate, 25, 1453–1469, doi: 10.1175/JCLI-D-11-00197.1, 2012.

Gordon, N. D., Norris, J. R., Weaver, C. P. and Klein, S. A.: Cluster analysis of cloud regimes and characteristic dynamics of midlatitude synoptic systems in observations and a model, J. Geophys. Res., 110, D15S17, doi: 10.1029/2004JD005027, 2005.

Grenier, H. and Bretherton, C. S.: A moist parametrization for large-scale models and its application to subtropical cloud-topped marine boundary layers, Mon. Weather Rev., 129, 357–377, doi: 10.1175/1520-0493(2001)129<0357:AMPPFL>2.0.CO;2, 2001.

Hansen, J., Sato, M., Ruedy, R., Nazarenko, L., Lacis, A., Schmidt, G. A., Russell, G., Aleinov, I., Bauer, M., Bauer, S., Bell, N., Cairns, B., Canuto, V., Chandler, M., Cheng, Y., Del Genio, A., Faluvegi, G., Fleming, E., Friend, A., Hall, T., Jackman, C., Kelley, M., Kiang, N., Koch, D., Lean, J., Lerner, J., Lo, K., Menon, S., Miller, R., Minnis, P., Novakov, T., Oinas, V., Perlwitz, J., Rind, D., Romanou, A., Shindell, D., Stone, P., Sun, S., Tausnev, N., Thresher, D., Wielicki, B., Wong, T., Yao, M., and Zhang, S.: Efficacy of climate forcings, J. Geophys. Res., 110, D18104, doi: 10.1029/2005JD005776, 2005.

Hannay, C., Williamson, D. L., Hack, J. J., Kiehl, J. T., Olson, J. G., Klein, S. A., Bretherton, C. S. and Köhler M.: Evaluation of Forecasted Southeast Pacific Stratocumulus in the NCAR, GFDL, and ECMWF Models, J. Climate, 22, 2871–2889, doi: 10.1175/2008JCLI2479.1, 2009.

Haywood, J. M., Donner, L. J., Jones, A., and Golaz, J.-C.: Global indirect radiative forcing caused by aerosols: IPCC (2007) and beyond, in: Clouds in the Perturbed Climate System, edited by: Heintzenberg, J. and Charlson, R. J., MIT Press, Cambridge, 451–467, 2009.

Holtslag, A. A. M., Svensson, G., Baas, P., Basu, S., Beare, B., Beljaars, A. C. M., Bosveld, F. C., Cuxart, J., Lindvall, J., Steeneveld, G. J., Tjernström, M. and Van De Wiel B. J. H.: Stable atmospheric boundary layers and diurnal cycles - challenges for weather and climate models. B. Am. Meteorol. Soc., 88, doi: 10.1175/BAMS-D-11-00187.1, 2013.

Hoose, C. Lohmann, U., Bennartz, R., Croft, B. and Lesins, G.: Global simulations of aerosol processing in clouds. Atmos. Chem. Phys., 8, 6939-6963, doi: 10.5194/acp-8-6939-2008, 2008a.

Hoose, C., Lohmann, U., Stier, P., Verheggen, B. and Weingartner, E.: Aerosol processing in mixed-phase clouds in ECHAM5-HAM: Model description and comparison to observations, J. Geophys. Res., 113, D07210, doi: 10.1029/2007JD009251, 2008b.

Isotta, F. A., Spichtinger, P., Lohmann, U. and von Salzen K.: Improvement and Implementation of a Parameterization for Shallow Cumulus in the Global Climate Model ECHAM5-HAM, J. Atmos. Sci., 68, 515-532, doi:10.1175/2010JAS3447.1, 2011.

Jakob, C. and Tselioudis, G.: Objective identification of cloud regimes in the Tropical Western Pacific, Geophys. Res. Lett., 30, doi: 10.1029/2003GL018367, 2003.

Joos, H., Spichtinger, P. and Lohmann, U.: Influence of a future climate on the microphysical and optical properties of orographic cirrus clouds in ECHAM5, J. Geophys. Res., 115, D19129, doi: 10.1029/2010JD013824, 2010.

Khairoutdinov, M. and Kogan, Y.: A new cloud physics parameterization in a large-eddy simulation model of marine stratocumulus, Mon. Weather Rev., 128, 229–243,doi: 10.1175/1520-0493(2000)128<0229:ANCPPI>2.0.CO;2, 2000.

King, M. D., Menzel, W. P., Kaufman, Y. J., Tanré, D., Gao, B. C., Platnick, S., Ackerman, S. A., Remer, L. A., Pincus, R. and Hubanks, P. A.: Cloud and aerosol properties, precipitable water, and profiles of temperature and humidity from MODIS, IEEE T. Geosci. Remote, 41, 442–458, doi: 10.1109/TGRS.2002.808226, 2003.

King, J. C., Connolley, W. M., Derbyshire and S. H.: Sensitivity of modelled Antarctic climate to surface and boundary-layer flux parametrizations, Q. J. Roy. Meteor. Soc., 127, 779-794, doi: 10.1256/smsqj.57303, 2001.

Koehler, M.,: Improved prediction of boundary layer clouds. ECMWF Newsletter, No. 104, ECMWF, Reading, United Kingdom, 18–22. [Available online at http://www.ecmwf.int/publications/newsletters/pdf/104.pdf.], 2005.

Koehler, M., Ahlgrimm, M., and Beljaars A.: Unified treatment of dry convective and stratocumulus-topped boundary layers in the ECMWF model, Q. J. Roy. Meteor. Soc., 137, 43–57, doi: 10.1002/qj.713, 2011.

Lamarque, J., Bond, T., Eyring, V., Granier, C., Heil, A., Klimont, Z., Lee, D., Liousse, C., Mieville, A., Owen, B., Schultz, M., Shindell, D., Smith, S., Stehfest, E., Van Aardenne, J., Cooper, O., Kainuma, M., Mahowald, N., McConnell, J., Naik, V., Riahi, K., and van Vuuren, D.: Historical (1850–2000) gridded anthropogenic and biomass burning emissions of reactive gases and aerosols: methodology and application, Atmos. Chem. Phys., 10, 7017–7039, doi: 10.5194/acp-10-7017-2010, 2010.

Lenderink, G. and Holtslag, A. A. M.: Evaluation of the Kinetic Energy Approach for Modeling Turbulent Fluxes in Stratocumulus, Mon. Weather Rev., 128, 244-258, doi: 10.1175/1520-0493(2000)128<0244:EOTKEA>2.0.CO;2, 2000.

Loeb, N. G., Wielicki, B. A., Doelling, D. R., Smith, G. L., Keyes, D. F., Kato, S., Manalo-Smith, N. and Wong, T.: Towards Optimal Closure of the Earth’s Top-of-Atmosphere Radiation Budget, J. Climate, 22, 748–766, doi: 10.1175/2008JCLI2637.1, 2009.

Lohmann, U., Stier, P., Hoose, C., Ferrachat, S., Kloster, S., Roeckner, E. and Zhang, J.: Cloud microphysics and aerosol indirect effects in the global climate model ECHAM5-HAM, Atmos. Chem. Phys., 7, 3425-3446, doi: 10.5194/acp-7-3425-2007, 2007.

Lohmann, U. and Ferrachat, S.: Impact of parametric uncertainties on the present-day climate and on the anthropogenic aerosol effect, Atmos. Chem. Phys., 10, 11373-11383, doi: 10.5194/acp-10-11373-2010, 2010.

Lohmann, U., Rotstayn, L., Storelvmo, T., Jones, A., Menon, S., Quaas, J., Ekman, A. M. L., Koch, D., and Ruedy, R.: Total aerosol effect: radiative forcing or radiative flux perturbation?, Atmos. Chem. Phys., 10, 3235–3246, doi:10.5194/acp-10-3235-2010, 2010.

Martin, G. M. et al.: The HadGEM2 family of Met Office Unified Model climate configurations, Geosci. Model Dev., 4, 723–757, doi: 10.5194/gmd-4-723-2011, 2011.

Medeiros, B. and Stevens, B: Revealing differences in GCM representations of low clouds, Clim. Dynam., 36, 385-399, doi: 10.1007/s00382-009-0694-5, 2011.

Nam, C. C. W. and Quaas, J.: Geographically versus dynamically defined boundary layer cloud regimes and their use to evaluate general circulation model cloud parameterizations, Geophys. Res. Lett., 40, 5951-4956, doi: 10.1002/grl.50945, 2013.

Nam, C. C. W., Quaas, J., Neggers., R, Siegenthaler- Le Drian, C. and Isotta, F.: Evaluation of boundary layer cloud parameterizations in the ECHAM5 general circulation model using CALIPSO and CloudSat satellite data, J. Adv. Model. Earth Syst., accepted, doi: 10.1002/2013MS000277, 2014.

Norris, J. R. and Weaver, C. P.: Improved techniques for evaluating GCM cloudiness applied to the NCAR CCM3, J. Clim., 14, 2540–2550, 2001.

O’Dell, C. W., Wentz, F. J. and Bennartz, R.: Cloud Liquid Water Path from Satellite-Based Passive Microwave Observations: A New Climatology over the Global Oceans, J. Climate, 21, 1721–1739, doi: 10.1175/2007JCLI1958.1, 2008.

Petch, J. C., Willett, M., Wong, R. Y. and Woolnough, S. J.: Modelling suppressed and active convection. Comparing a numerical weather prediction, cloud-resolving and singlecolumn model, Q. J. Roy. Meteor. Soc., 133, 1087–1100, doi: 10.1002/qj.109, 2007.

Pithan, F. and Mauritsen, T.: The role of stably stratified turbulence in Climate, Proceedings, 2012, www.ecmwf.int/publications/library/ecpublications/_pdf/workshop/2011/GABLS/Posters.pdf.

Possner, A., Zubler, E., Fuhrer, O., Lohmann, U. and Schär, C.: A Case study in Modelling Low-lying Inversions and Stratocumulus Cloud Cover in the Bay of Biscay, 2014, submitted.

Roeckner, E., Buml, G., Bonaventura, L., Brokopf, R., Esch, M., Giorgetta, M., Hagemann, S., Kirchner, I., Kornblueh, L., Manzini, E., Rhodin, A., Schlese, U., Schulzweida, U. and Tompkins, A.: The Atmospheric General Circulation Model ECHAM5: Part 1. REPORT 349, ISSN 0937-1060, Tech. rep., Max Planck Institute for Meteorology Hamburg, Germany, 2003.

Rossow, W. B. and Schiffer, R. A.: Advances in understanding clouds from ISCCP, B. Am. Meteorol. Soc., 80, 2261–2287, doi: 10.1175/1520-0477(1999)080<2261:AIUCFI>2.0.CO;2, 1999.

Sandu, I., Beljaars, A., Bechtold, P., Mauritsen, T. and Balsamo, G.: Why is it so difficult to represent stably stratified conditions in numerical weather prediction NWP models? J. Adv. Model. Earth Syst., 5, 117-133, doi: 10.1002/jame.20013, 2013.

Siegenthaler-Le Drian, C., Stratocumulus clouds in ECHAM5-HAM, Ph. D., ETH Zurich, Zurich, doi: 10.3929/ethz-a-006073454, 2010.

Stephens, G. L.: Cloud Feedbacks in the Climate System, J. Climate, 18, 237-273, doi: 10.1175/JCLI-3243.1, 2005.

Stevens, B., Moeng, C.-H., Sullivan and P. S.: Large-Eddy Simulations of Radiatively Driven Convection: Sensitivities to the Representation of Small Scales, J. Atmos. Sci., 56, 3963-3984, doi: 10.1175/1520-0469(1999)056<3963:LESORD>2.0.CO;2, 1999.

Stevens, B., Beljaars, A., Bordoni, S., Holloway, C., Koehler, M., Krueger, S., Savic-Jovcic, V. and Zhang, Y.: On the structure of the lower troposphere in the summertime stratocumulus regime of the northeast Pacific, Mon. Weather Rev., 135, 985–1005, doi: 10.1175/MWR3427.1, 2007.

Stevens, B., Giorgetta, M., Esch, M., Mauritsen, T., Crueger, T., Rast, S., Salzmann, M., Schmidt, H., Bader, J., Block, K., Brokopf, R., Fast, I., Kinne, S., Kornblueh, L., Lohmann, U., Pincus, R., Reichler, T. and Roeckner, E.: Atmospheric component of the MPI-M Earth

System Model: ECHAM6, J. Adv. Model. Earth Syst., 5, 146-172, doi: 10.1002/jame.20015, 2013.

Stier, P., Feichter, J., Kinne, S., Kloster, S., Vignati, E., Wilson, J., Ganzeveld, L., Tegen, I., Werner, M., Balkanski, Y., Schulz, M., Boucher, O., Minikin, A. and Petzold, A.: The aerosol-climate model ECHAM5-HAM, Atmos. Chem. Phys., 5, 1125–1156, doi: 10.5194/acp-5-1125-2005, 2005.

Sundqvist, H., Berge, E., and Kristiansson, J. E.: Condensation and Cloud Parameterization Studies with a Mesoscale Numerical Weather Prediction Model, Mon. Wea. Rev., 117, 1641–1657, doi: 10.1175/1520-0493(1989)117<1641:CACPSW>2.0.CO;2, 1989.

Tiedtke, M.: A comprehensive mass flux scheme for cumulus parameterization in large-scale models, Mon. Weather Rev., 117, 1779-1800., doi: 10.1175/1520-0493(1989)117<1779:ACMFSF>2.0.CO;2, 1989.

Tselioudis, G., Zhang, Y. and Rossow, W. B.: Cloud and radiation variations associated with northern midlatitude low and high sea level pressure regimes. J. Clim., 13, 312–327, 2000.

Tselioudis, G. and Jakob, C.: Evaluation of midlatitude cloud properties in a weather and a climate model: dependence on dynamic regime and spatial resolution, J. Geophys. Res., 107(D24), 4781, doi: 10.1029/2002JD002259, 2002.

Tsushima, Y., Ringer, M. A., Webb, M. J. and Williams, K. D.: Quantitative evaluation of the seasonal variations in climate model regimes, Clim. Dynam., 41, 2679-2696, doi: 10.1007/s00382-012-1609-4, 2013.

Williams, K. D., Ringer, M. A., Senior, C. A., Webb, M. J., McAvaney, B. J., Andronova, N., Bony, S., Dufresne, J. L., Emori, S., Gudgel, R., Knutson, T., Li, B., Lo, K., Musat, I., Wegner, J., Slingo, A. and Mitchell, J. F. B.: Evaluation of a component of the cloud response to climate change in an intercomparison of climate models, Clim. Dyn., 26, 145–165, doi:10.1007/s00382-005-0067-7, 2006.

Williams, K. D. and Tselioudis, G.: GCM intercomparison of global cloud regimes: present-day evaluation and climate change response, Clim. Dynam., 29, 231–250, doi:10.1007/s00382-007-0232-2, 2007.

Williams, K. D. and Webb, M. J.: A quantitative performance assessment of cloud regimes in climate models, Clim. Dynam., 33, 141-157, doi: 10.1007/s00382-008-0443-1, 2009.

Winker, D. M. and Coauthors: The CALIPSO mission: A global 3D view of aerosols and clouds, B. Am. Meteorol. Soc., 91, 1211–1229, 2010.

Wood, R., Bretherton, C. S. and Hartmann, D. L.: Diurnal cycle of liquid water path over the subtropical and tropical oceans, Geophys. Res. Lett., 29, 2092, doi: 10.1029/2002GL015371, 2002.

Wyant, M. C., Bretherton, C. S., Chlond, A., Griffin, B. M., Kitagawa, H., Lappen, C., Larson, V. E., Lock A., Park, S., de Roode, S. R., Uchida, J., Zhao, M. and Ackerman, A. S.: A single-column model intercomparison of a heavily drizzling stratocumulus-topped boundary layer, J. Geophys. Res., 112, D24204, doi: 10.1029/2007JD008536, 2007.

Xue H, and Feingold G.: Large-eddy simulations of trade wind cumuli: Investigation of aerosol indirect effects, J. Atmos. Sci., 63, 1605–1622, doi: 10.1175/JAS3706.1, 2006.

Zhang, Y., Klein, S., Mace, G. G. and Boyle, J.: Cluster analysis of tropical clouds using CloudSat data, Geophys. Res. Lett., 34, L12813, doi:10.1029/2007GL029336, 2007.

Zhang, K., O'Donnel, D., Kazil, J., Stier., P., Kinne, S., Lohmann, U., Ferrachat, S., Croft, B., Quaas, J., Wan, H., Rast, S. and Feichter, J.: The global aerosol-climate model ECHAM-HAM, version 2: sensitivity to improvements in process representations, Atmos. Chem. Phys., 12, 8911-8949, doi: 10.5194/acp-12-8911-2012, 2012.

Zhang, M. et al.: CGILS: Results from the first phase of an international project to understand the physical mechanisms of low cloud feedbacks in single column models, J. Adv. Model. Earth Syst., 5, 1-17, doi: 10.1002/2013MS000246, 2013.

Zhu, P., Bretherton, C. S., Kohler, M., Cheng, A. N., Chlond, A., Geng, Q. Z. , Austin, P., Golaz, J. C., Lenderink, G., Lock, A. and Stevens, B.: Intercomparison and interpretation of single-column model simulations of a nocturnal stratocumulus-topped marine boundary layer, Mon. Weather Rev., 133, 2741-2758, doi: 10.1175/MWR2997.1, 2005.

Zygmuntowska, M., Mauritsen, T., Quaas, J. and Kaleschke L.: Arctic Clouds and Surface Radiation – a critical comparison of satellite retrievals and the ERA-Interim reanalysis, Atmos. Chem. Phys., 12, 6667-6677, doi: 10.5194/acp-12-6667-2012, 2012.

Table 1. Description of experiments conducted in this study.

Label	Vertical Resolution	Tuning factor of the autoconversion rate (ccraut)	Description	Sea surface temperature and sea ice over	Other changes
REF	L31	4	control simulation	AMIP/CLIM	
STAB	L31	3.5	modified stability function	AMIP/CLIM	
VRES47	L47bl	4	additional model levels (47 levels in total)	AMIP/CLIM	Reduced entrainment deep convective clouds
VRES95	L95bl	12	additional model levels (95 levels in total)	AMIP/CLIM	Reduced entrainment deep convective clouds
AP	L31	5	in-cloud aerosol processing	AMIP/CLIM	
STAB+AP	L31	5	STAB+AP	AMIP/CLIM	Tuning as STAB
VRES47+ STAB	L47bl	4	VRES47+STAB	AMIP/CLIM	Tuning as VRES47
NOPRECIP	L31	4	Sc-precipitation turned off	CLIM	
NOSHCV	L31	4	shallow convective cloud parameterization turned off	CLIM	

Table 2. Aerosol, cloud and forcing parameters for present day CLIM simulations for all experiments. Global values and values in the stratocumulus regime are given. Note that the results with L47bl and L95bl are from one year simulations. LWP is liquid water path, IWP is ice water path, N_d and N_i refer to the vertically integrated cloud droplet and ice crystal number concentration, (L)CC is (low) cloud cover, $P_{tot}/P_{strat}/P_{conv}$ are total/stratiform/convective precipitation, SCF is shortwave cloud forcing and AOD the aerosol optical depth. Global annual mean burdens for sulfate (SO_4), black carbon (BC), organic carbon (OC), sea salt (SS) and mineral dust (DU). The subscript $_{Sc}$ represents values in the stratocumulus regime.

Variable	Experiment (PD)						
	REF	STAB	AP	STAB +AP	VRES47	VRES95	VRES47 +STAB
LWP (g/m^2)	85.3	83.3	77.9	81.9	91.1	74.2	85.4
IWP (g/m^2)	10.4	10.3	10.5	10.5	11.6	9.8	11.6
N_d ($10^{10}/m^2$)	3.2	2.9	2.9	2.6	3.5	3.8	3.1
N_i ($10^{10}/m^2$)	0.2	0.2	0.2	0.2	0.2	0.1	0.2
CC	63.8	64.3	63.5	64.1	64.4	66.6	63.3
P_{tot} (mm/d)	2.98	2.94	2.99	2.94	3.03	3.17	3.00
P_{strat} (mm/d)	1.56	1.52	1.57	1.52	1.07	1.06	1.04
P_{conv} (mm/d)	1.42	1.42	1.42	1.43	1.96	2.11	1.97
Net rad. TOA (W/m^2)	0.18	0.28	-0.97	-1.39	-0.19	-0.36	0.94
AOD (@550nm)	0.125	0.122	0.328	0.287	0.097	0.085	0.099
SO_4 burden (Tg)	1.82	1.87	1.45	1.47	1.90	1.74	1.93
BC burden (Tg)	0.14	0.14	0.10	0.10	0.11	0.09	0.11
OC burden (Tg)	1.07	1.07	0.88	0.89	0.82	0.64	0.81
SS burden (Tg)	10.8	10.4	18.2	16.3	9.3	7.4	9.1
DU burden (Tg)	11.6	11.7	12.4	15.0	5.6	7.4	8.2
LWP_{Sc} (g/m^2)	73.1	82.3	73.6	88.3	71.6	74.9	67.2
LCC_{Sc}	47.5	52.8	47.5	52.3	38.4	54.9	38.3
SCF_{Sc} (W/m^2)	-58.9	-63.2	-58.1	-63.5	-54.7	-72.2	-51.4
AOD_{Sc} (@550nm)	0.110	0.101	0.342	0.272	0.111	0.125	0.111

Table 3. Changes in aerosol, cloud and forcing parameters between simulations with pre-industrial and present day aerosol for all experiments. Global values and values in the stratocumulus regime are given. Note that the results with L47bl and L95bl are from one year simulations. LWP is liquid water path, CC is cloud cover, AAE is the anthropogenic aerosol effect, τ_{anth} the anthropogenic aerosol optical depth and $\Delta\tau$ the change in aerosol optical. The subscript $_{Sc}$ represents values in the stratocumulus regime. Values marked by * are not statistically significant or could not be tested for statistical significance.

Variable	Experiment (PD-PIaer)						
	REF	STAB	AP	STAB +AP	VRES47	VRES95	VRES47 +STAB
ΔLWP (g/m^2)	6.5	6.4	5.0	4.4	9.3	7.4	8.5
ΔCC	0.5	0.4	0.3	0.2	1.2	0.9	0.7
AAE (W/m^2)	-1.19	-1.34	-1.08	-0.90	-2.08	-2.32	-1.89
AAE_{SW} (W/m^2)	-2.12	-2.09	-1.72	-1.36	-3.41	-3.51	-3.03
AAE_{LW} (W/m^2)	0.94	0.75	0.65	0.46	1.33	1.19	1.14
τ_{anth} (@550nm)	0.019	0.018	0.026	0.012	0.013	0.012	0.018
ΔLWP_{Sc} (g/m^2)	6.6	9.5	5.3	2.8*	9.9*	12.6*	10.5*
AAE_{Sc} (W/m^2)	-2.95	-3.55	-2.90	-2.17*	-3.60*	-7.78*	-3.52*
$AAE_{Sc/SW}$ (W/m^2)	-2.95	-4.49	-2.69*	-1.81*	-5.08*	-7.48*	-4.01*
$\Delta\tau_{Sc}$ (@550nm)	0.006	0.009	0.010	0.000	0.000*	-0.009*	0.025*

Table B1. Probability computed with an unpaired two tails t-test with unequal variances applied to annual mean values of the present day and pre-industrial aerosol (climatological) simulations of an experiment that the differences between present day and pre-industrial aerosol simulations are not occurring by chance. AAE is the anthropogenic aerosol effect, LWP is liquid water path, τ is aerosol optical depth and Δ represents the difference between present-day and pre-industrial aerosol emissions. The subscript $_{Sc}$ represents values in the stratocumulus regime. Values < 90% are considered not statistically significant.

Variable	Experiment (PD-PIaer)			
	REF	STAB	AP	STAB +AP
AAE_{Sc}	91%	98%	91%	69%
$AAE_{Sc/SW}$	91%	98%	88%	56%
ΔLWP_{Sc}	100%	100%	100%	89%
$\Delta \tau_{Sc}$	100%	100%	100%	100%

Table B2. Same as Table B1 but the t-test is applied to annual mean values of (AMIP) simulations of an experiment and the reference experiment. CC stands for cloud cover, SWCRE for shortwave cloud radiative effect, subscript PD for present day aerosol emissions and PIaer for pre-industrial aerosol emissions.

Variable	Experiment (-REF)		
	STAB	AP	STAB +AP
CC_{PD}	100%	27%	98%
CC_{PIaer}	100%	38%	100%
LWP_{PD}	99%	32%	100%
LWP_{PIaer}	100%	92%	100%
$SWCRE_{PD}$	90%	28%	99%
$SWCRE_{PIaer}$	98%	16%	100%

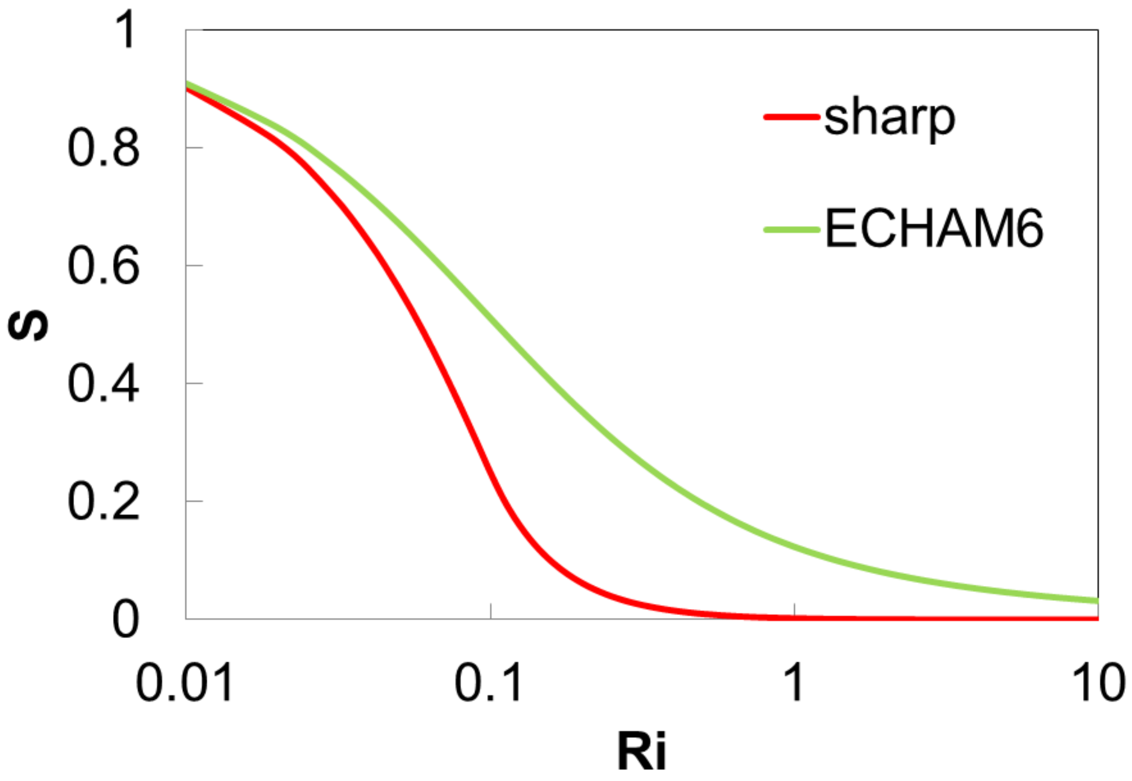

Figure 1. Comparison of ‘sharp’ and ECHAM6 stability function S (Eq. 4; dimensionless) as a function of Richardson number (Ri).

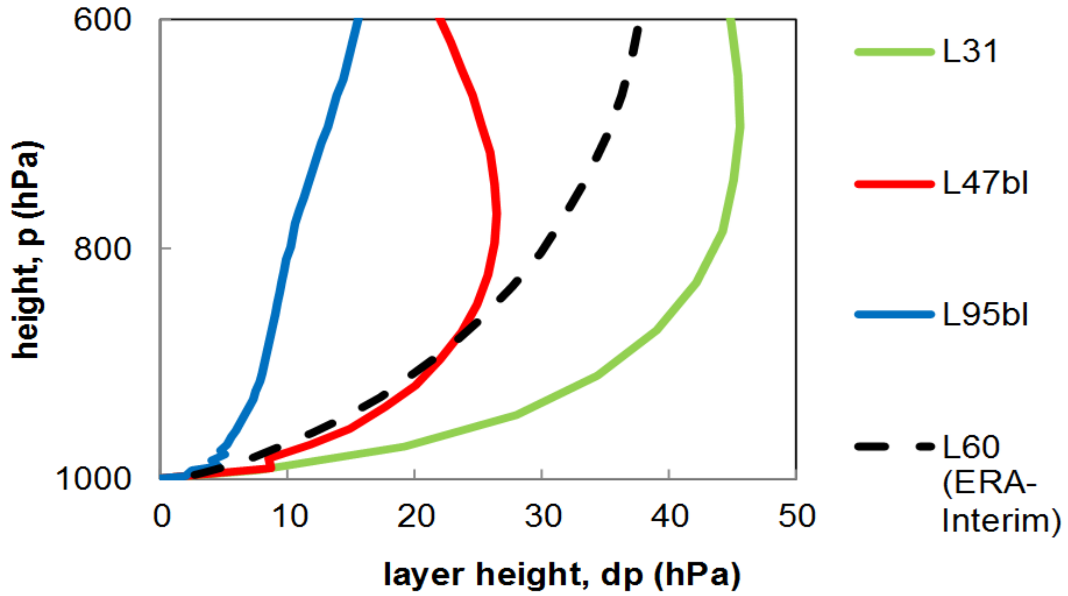

Figure 2. Vertical resolution of the reference L31 vertical grid and new L47bl and L95bl grids as well as the L60 vertical grid used in ERA-Interim. The (pressure) height of the model layers is shown as a function of the height above the surface for a surface pressure of 1000 hPa.

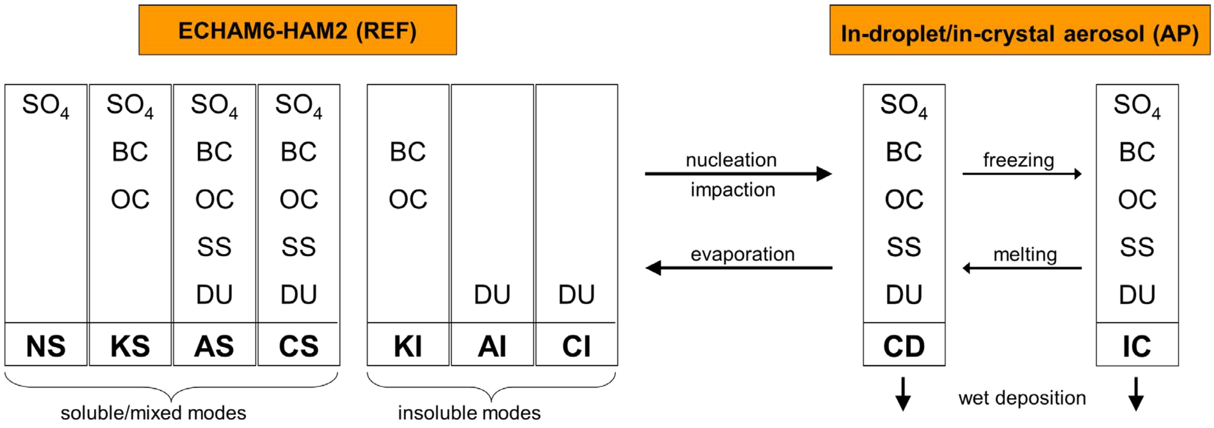

Figure 3. Processes and tracers used in the aerosol processing scheme. To the tracers for the soluble/mixed modes of HAM2 (nucleation (NS), Aitken (KS), accumulation (AS), coarse (CS)) and insoluble modes (Aitken (KI), accumulation (AI), coarse (CI)) new tracers for aerosol particles in cloud droplets (CD) and ice crystals (IC) are added.

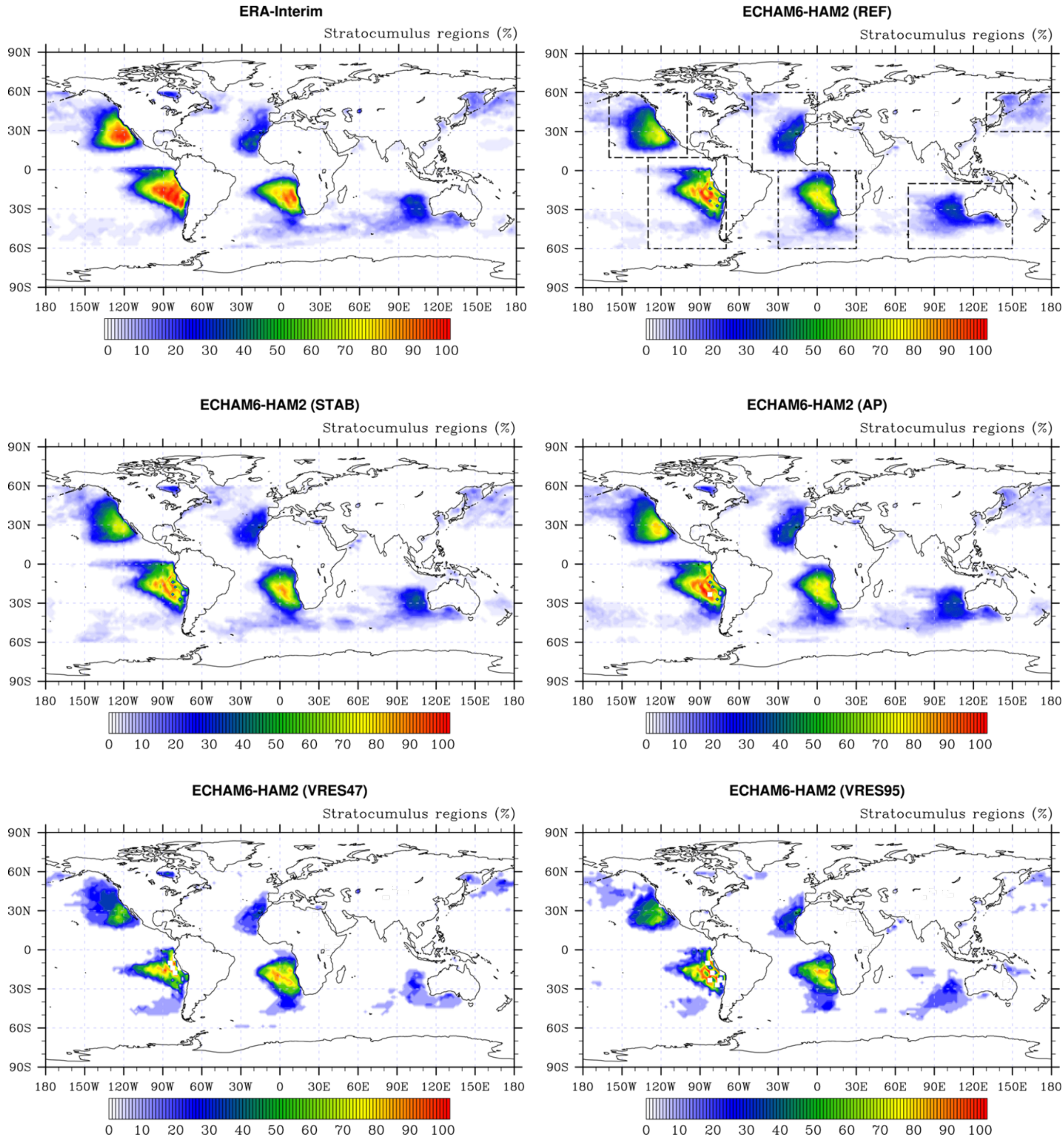

Figure 4. Frequency of occurrence of stratocumulus conditions in ERA-Interim and ECHAM6-HAM2 in the REF, STAB, AP, VRES47 and VRES95 experiments. In the panel for the REF experiment are also the six stratocumulus regions shown which are used in assessing the effect of anthropogenic aerosol.

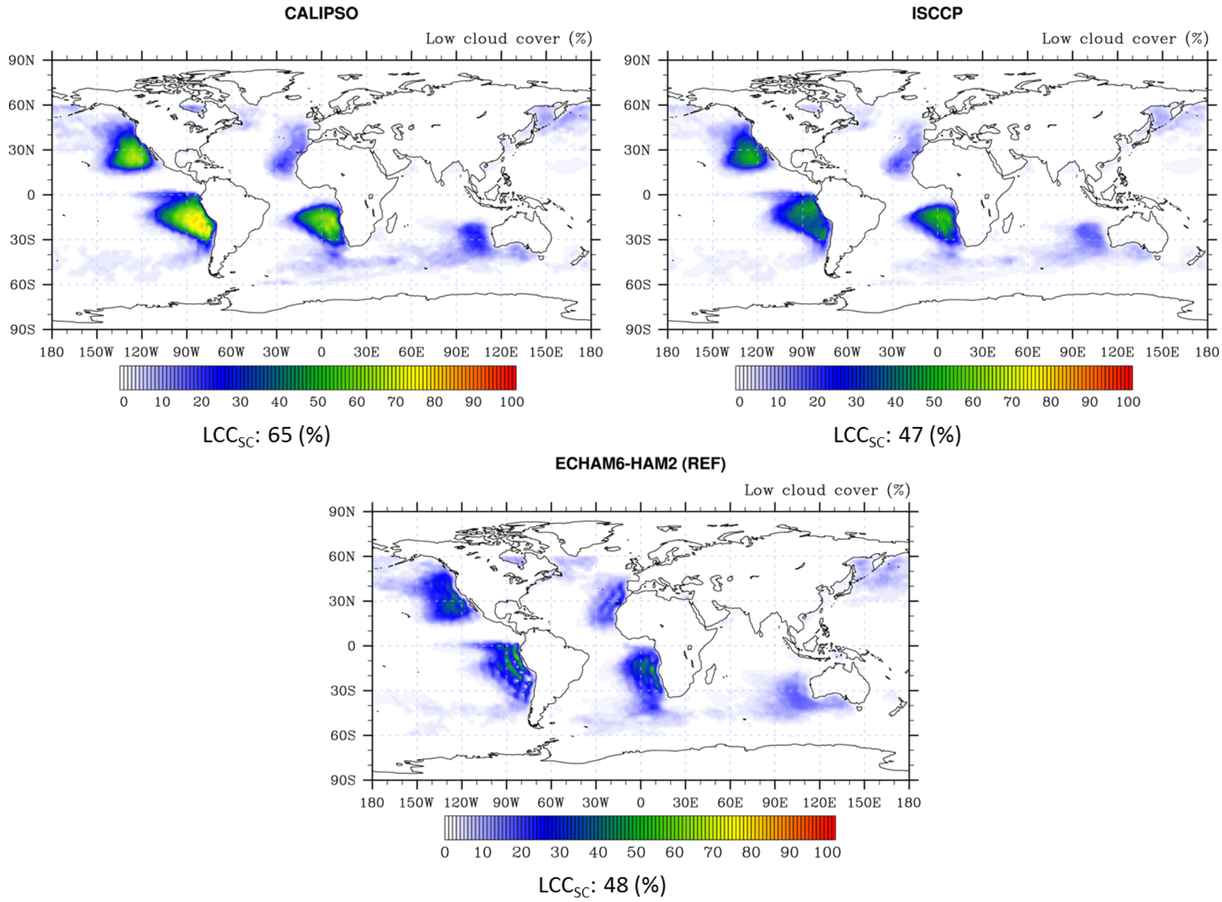

Figure 5. Low level cloud cover in stratocumulus cloud regions in the reference simulation and the CALIPSO and ISCCP satellite data. Values below each panel show in-regime values (subscript $_{SC}$). Note that in-regime values are larger than the mean over the stratocumulus cloud regions.

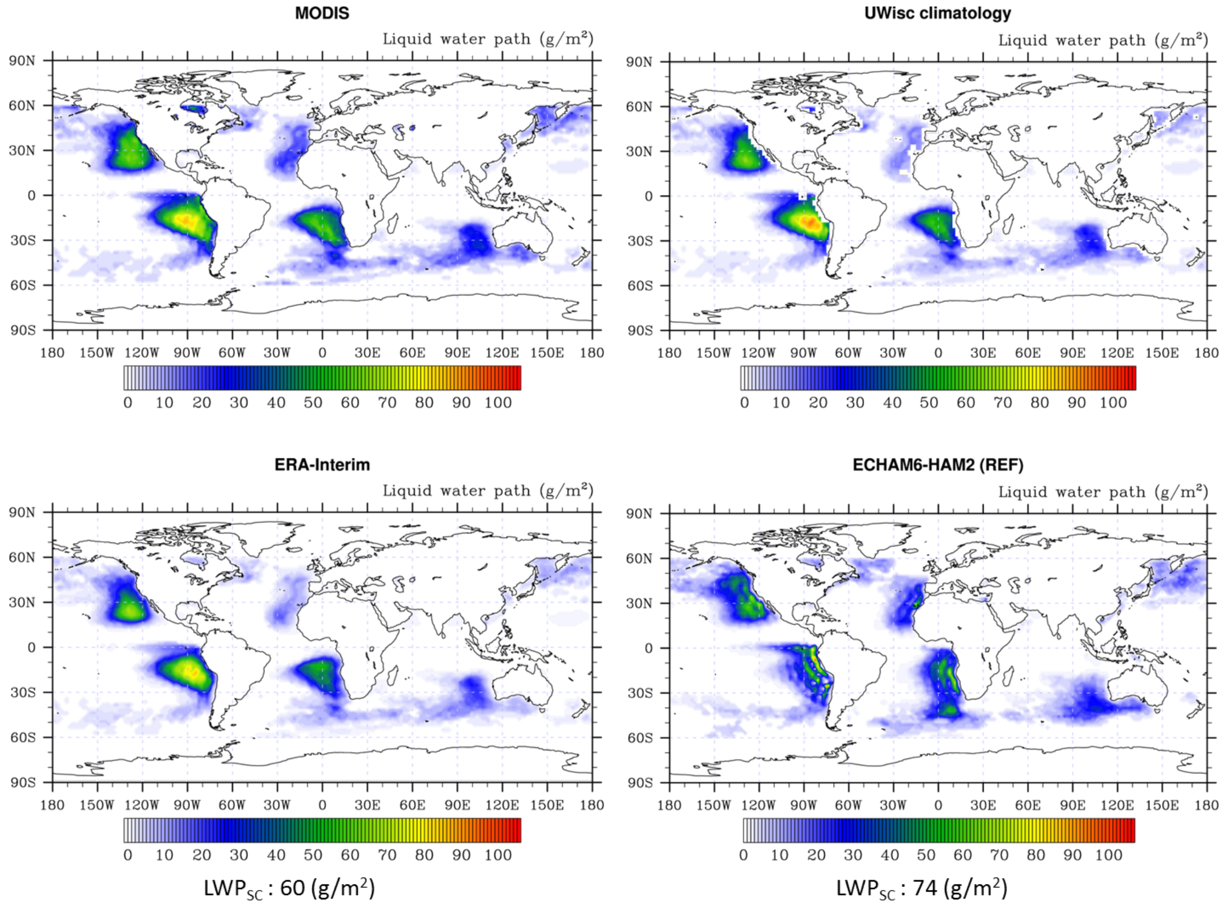

Figure 6. Liquid water path in stratocumulus cloud regions in the reference simulation, MODIS, ERA-Interim and a climatology from the University of Wisconsin. Values below the panels are in-regime values.

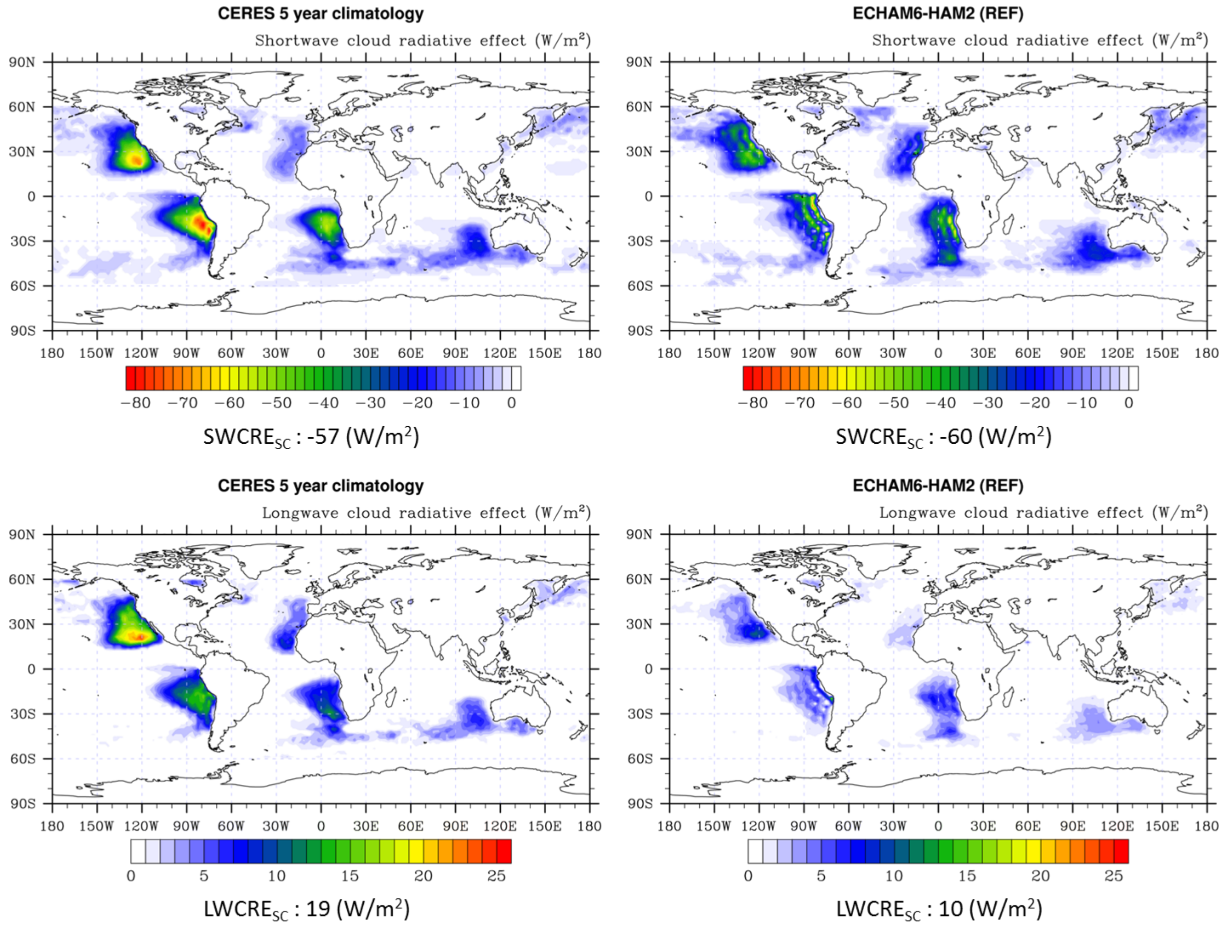

Figure 7. Shortwave and longwave cloud radiative effect in stratocumulus cloud regions in the reference simulation and a 5 years CERES climatology. Values below each panel are in-regime values.

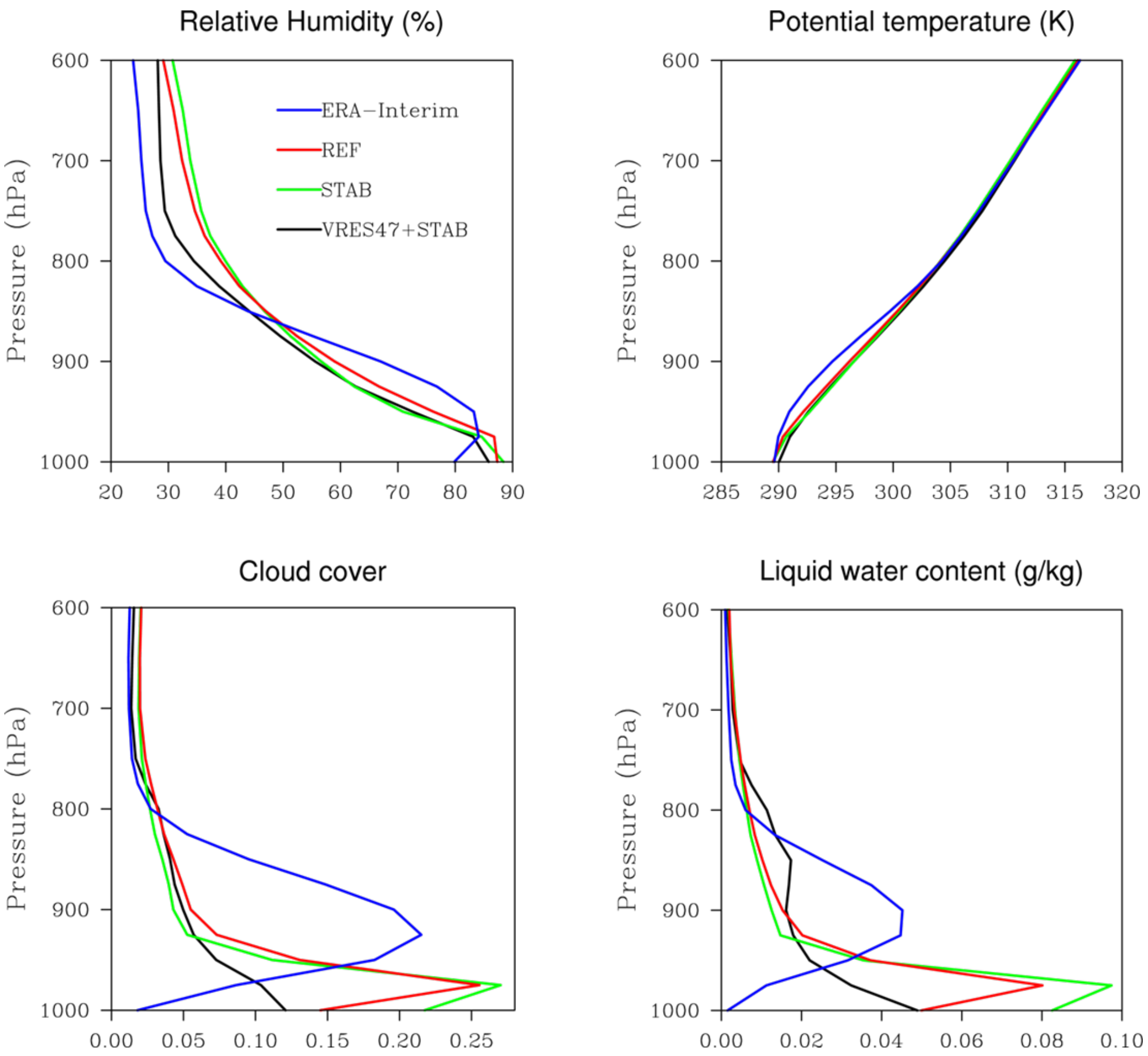

Figure 8. Vertical profiles of relative humidity, potential temperature, cloud cover and liquid water content in the stratocumulus regime. The red line is for the ECHAM6-HAM2 reference simulation, the green line for the STAB-simulation, the black line for the VRES47+STAB-simulation and the blue line for ERA-Interim data.

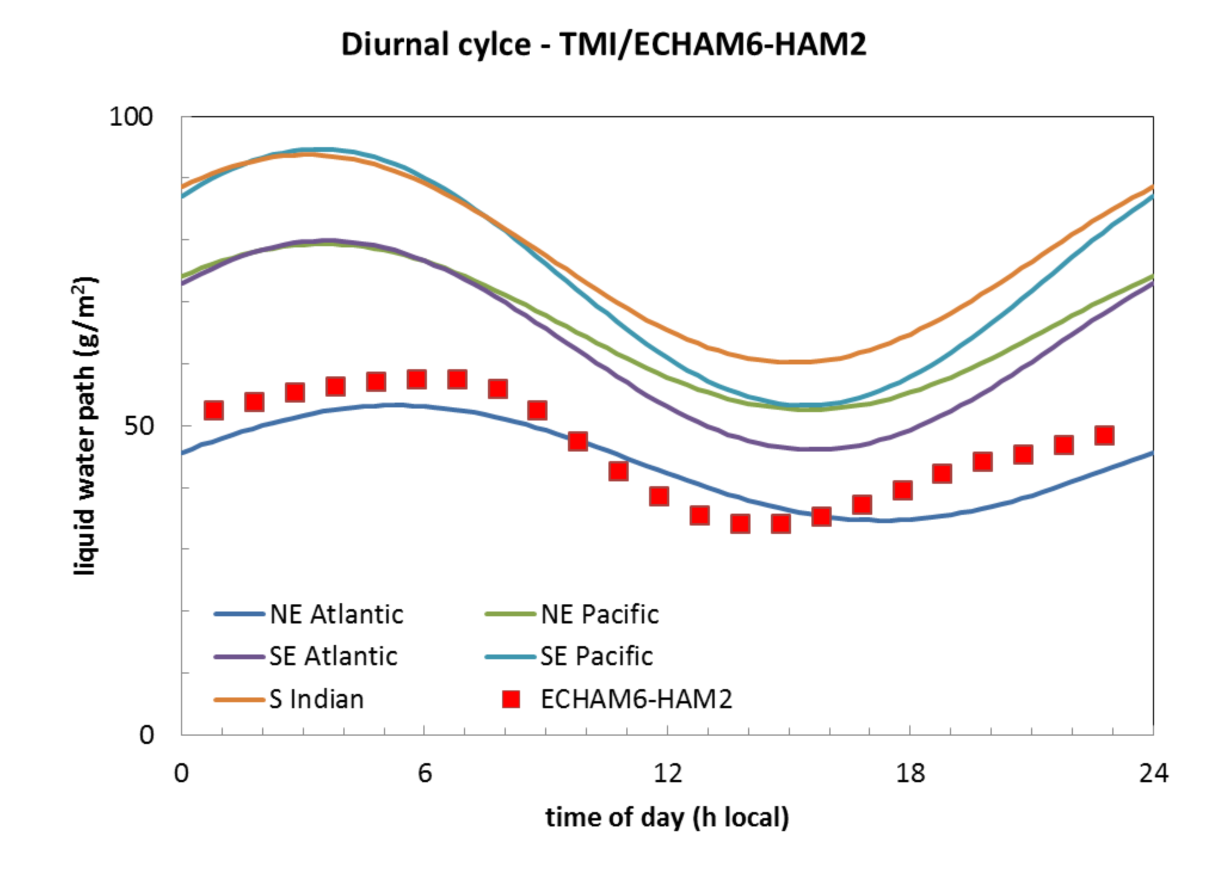

Figure 9. Diurnal cycle of liquid water path from TMI microwave radiometer data in different regions in 1999-2000 and ECHAM6-HAM2 in the stratocumulus regime in October 2006.

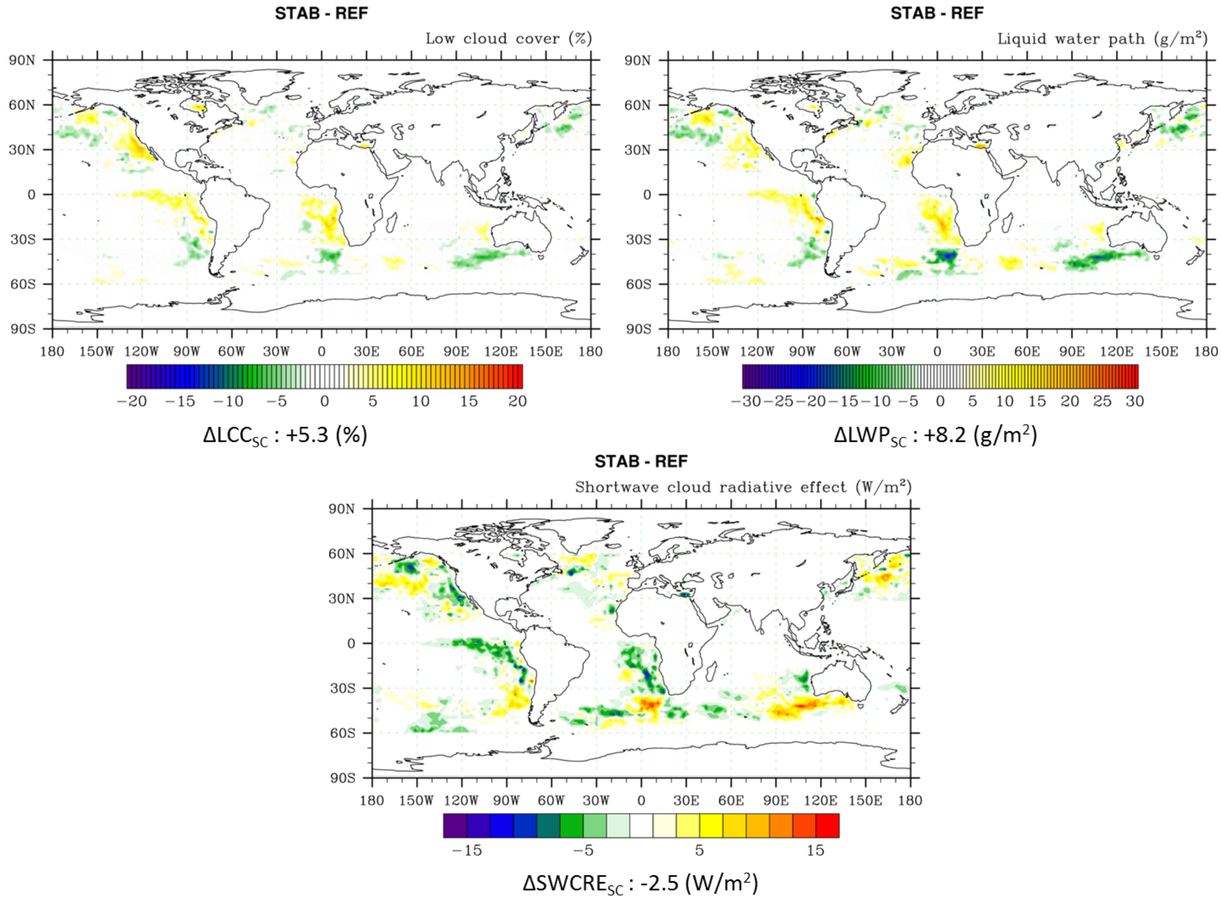

Figure 10. Difference in low cloud cover, LWP and SWCRE in stratocumulus regions between a simulation with a 'sharp' stability function and the reference simulation. Values below each panel are in-regime values.

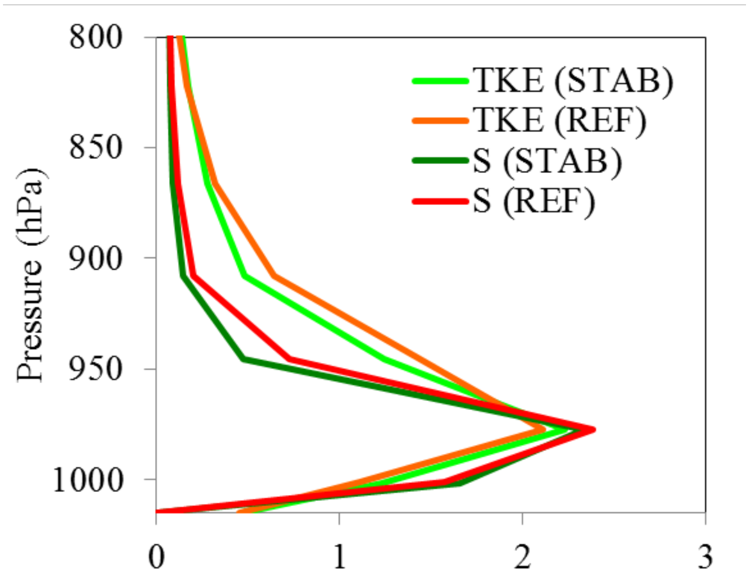

Figure 11. Vertical profiles of turbulent kinetic energy (TKE in m^2/s^2) and the stability function (dimensionless) are shown in the stratocumulus regime. The red and orange lines are for the ECHAM6-HAM2 reference simulation, the light and dark green lines for the STAB-simulation.

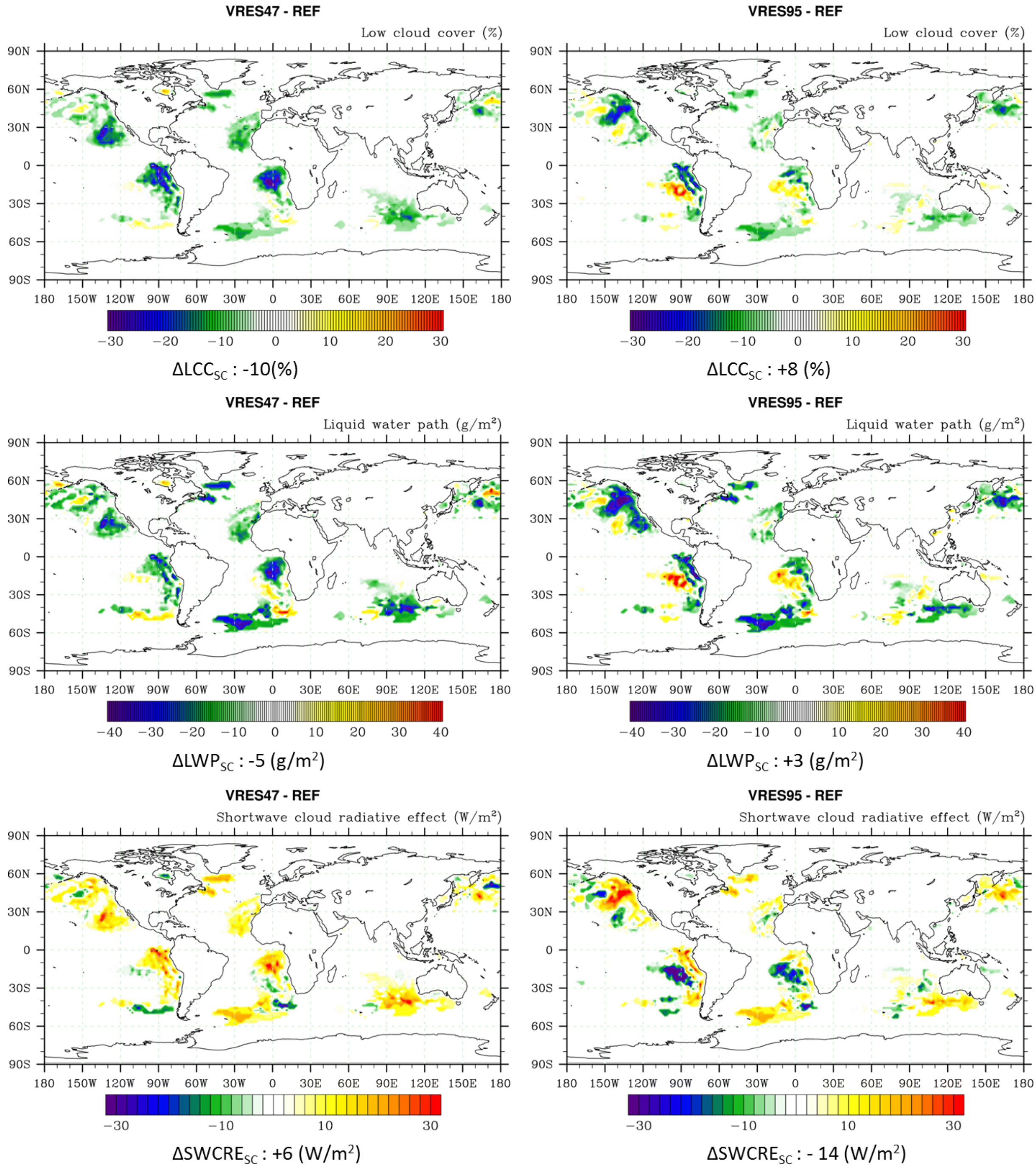

Figure 12. Same as in Fig. 10 but for increased vertical resolution (L47bl and L95bl). Values below each panel are in-regime values.

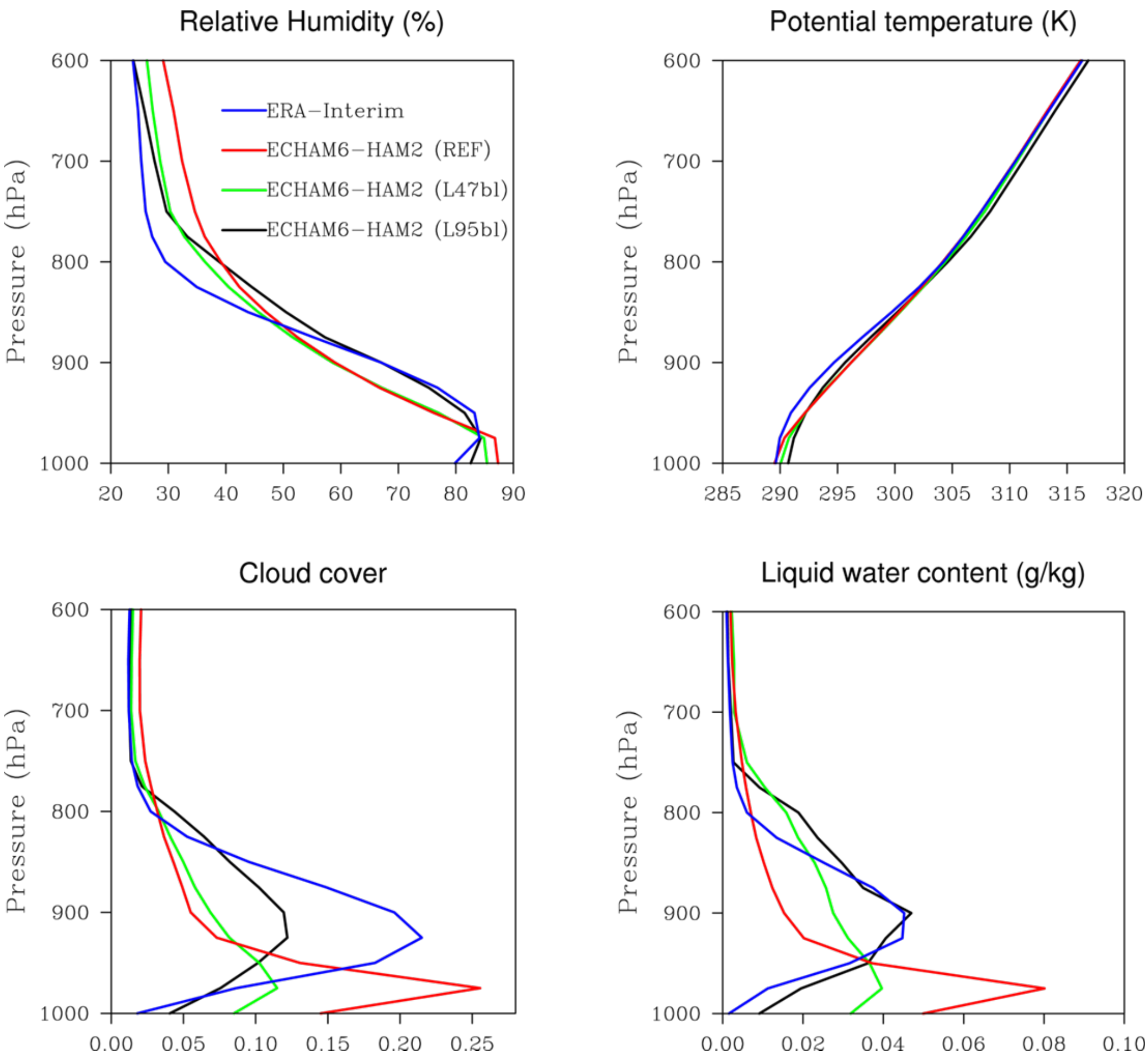

Figure 13. Vertical profiles of relative humidity, potential temperature, cloud cover and liquid water content in stratocumulus regions (in-regime values). The green line is for a simulation with the L47bl vertical grid, the black line for L95bl, the red line is for the ECHAM6-HAM2 reference simulation and the blue line for ERA-Interim data.

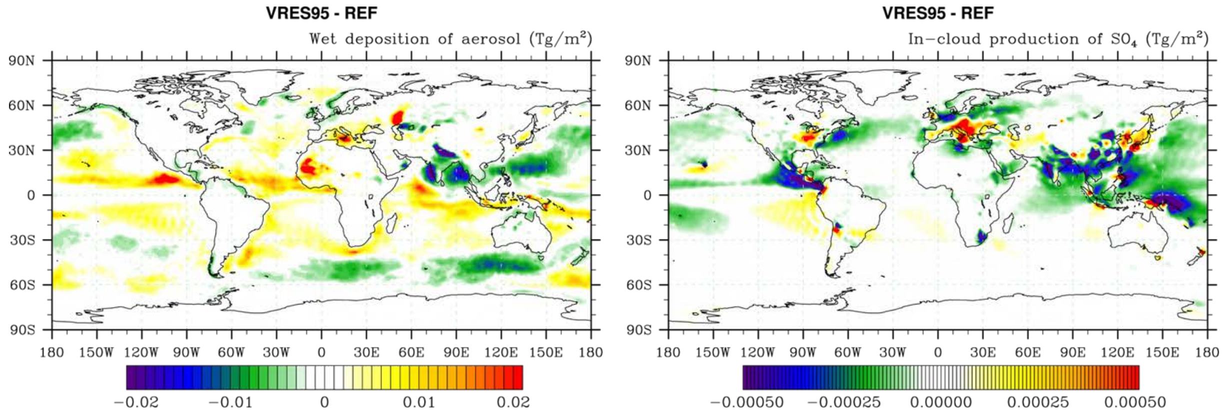

Figure 14. The change in wet deposition of aerosol mass and the change in production of SO_4 by wet chemistry between the VRES95 and the REF experiment are shown.

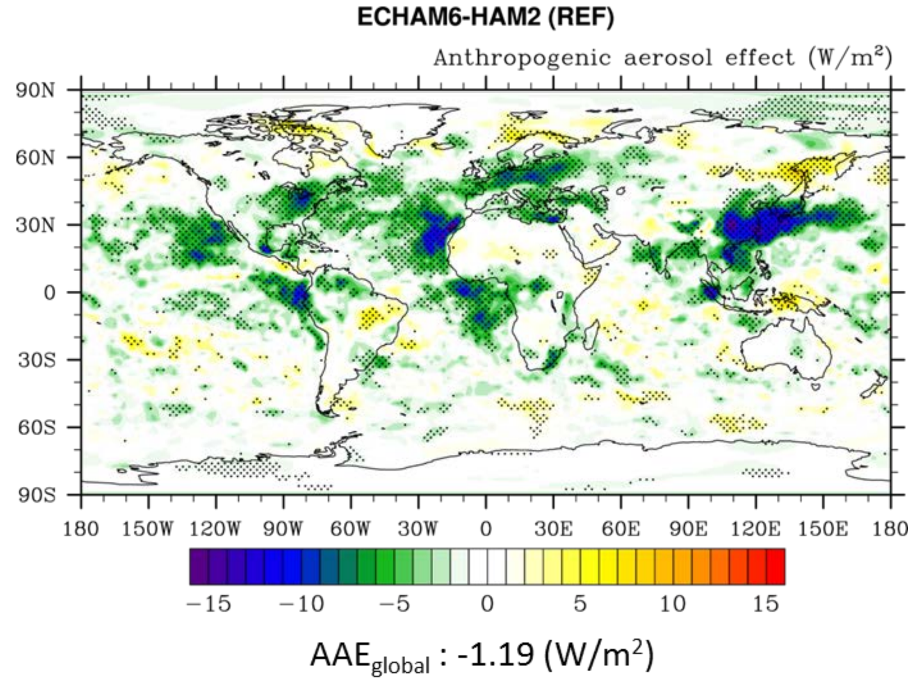

Figure 15. The total anthropogenfic aerosol effect (AAE) is shown globally. Below the panel the average value is shown.

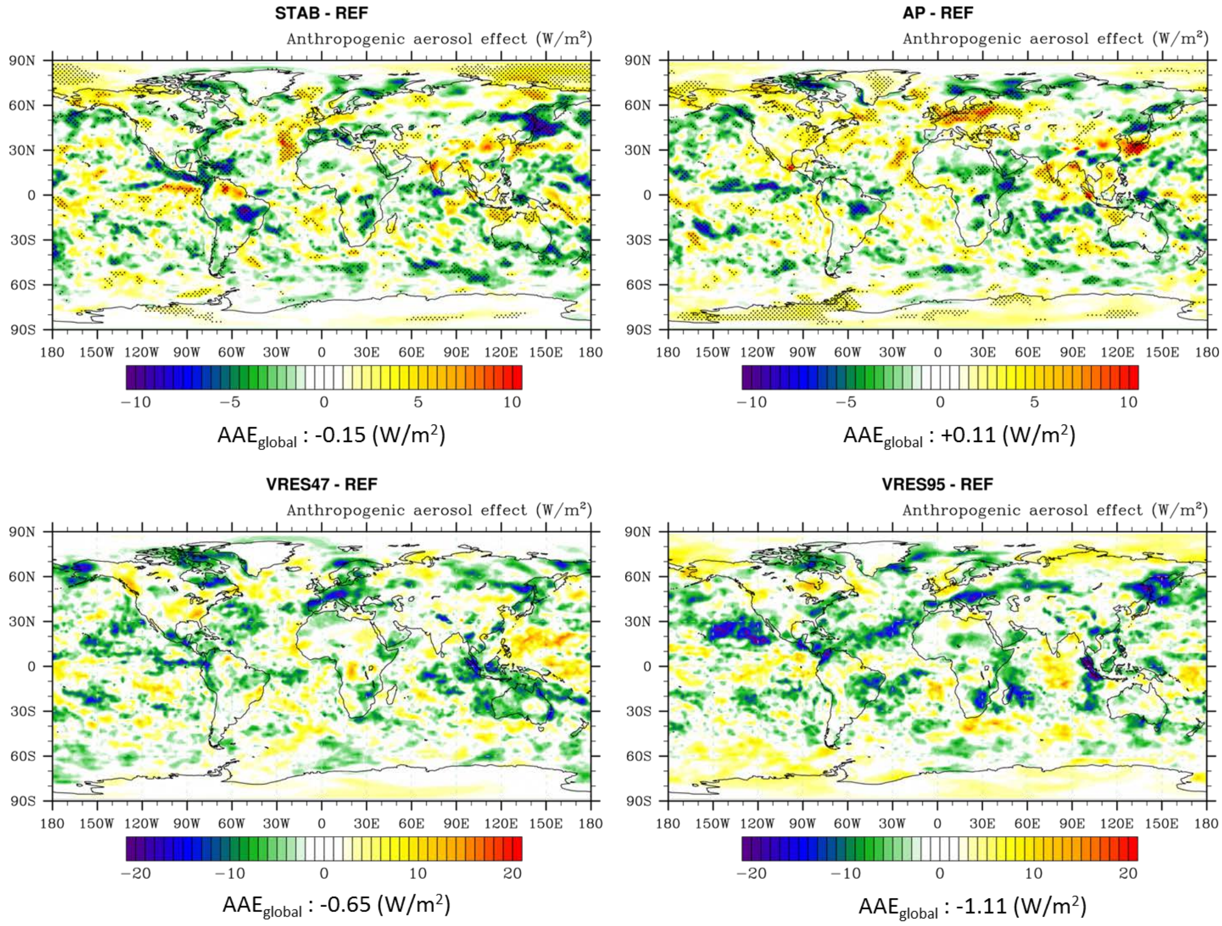

Figure 16. The change in *AAE* between the STAB, AP, VRES47 and VRES95 simulation and the reference simulation is shown globally. Values below each panel are average values for the areas above.

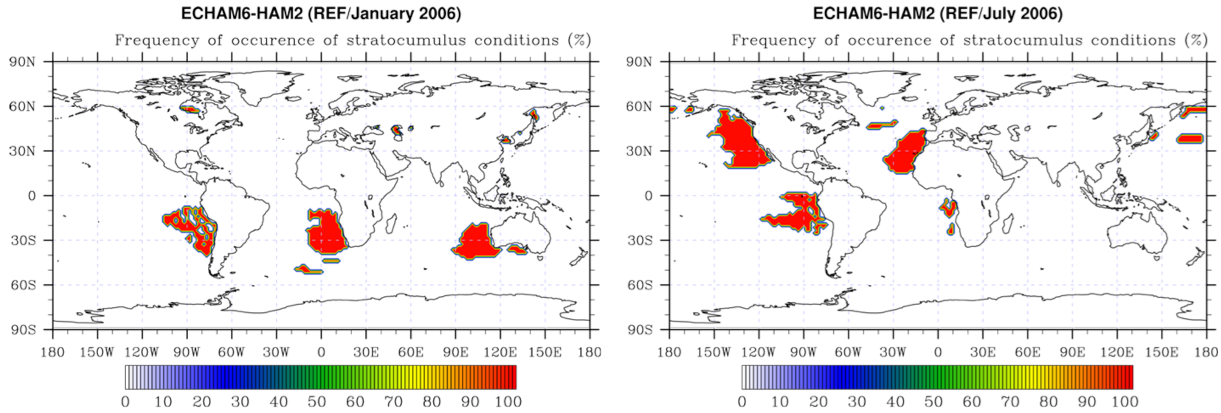

Figure A1. The stratocumulus regime in January and July 2006.

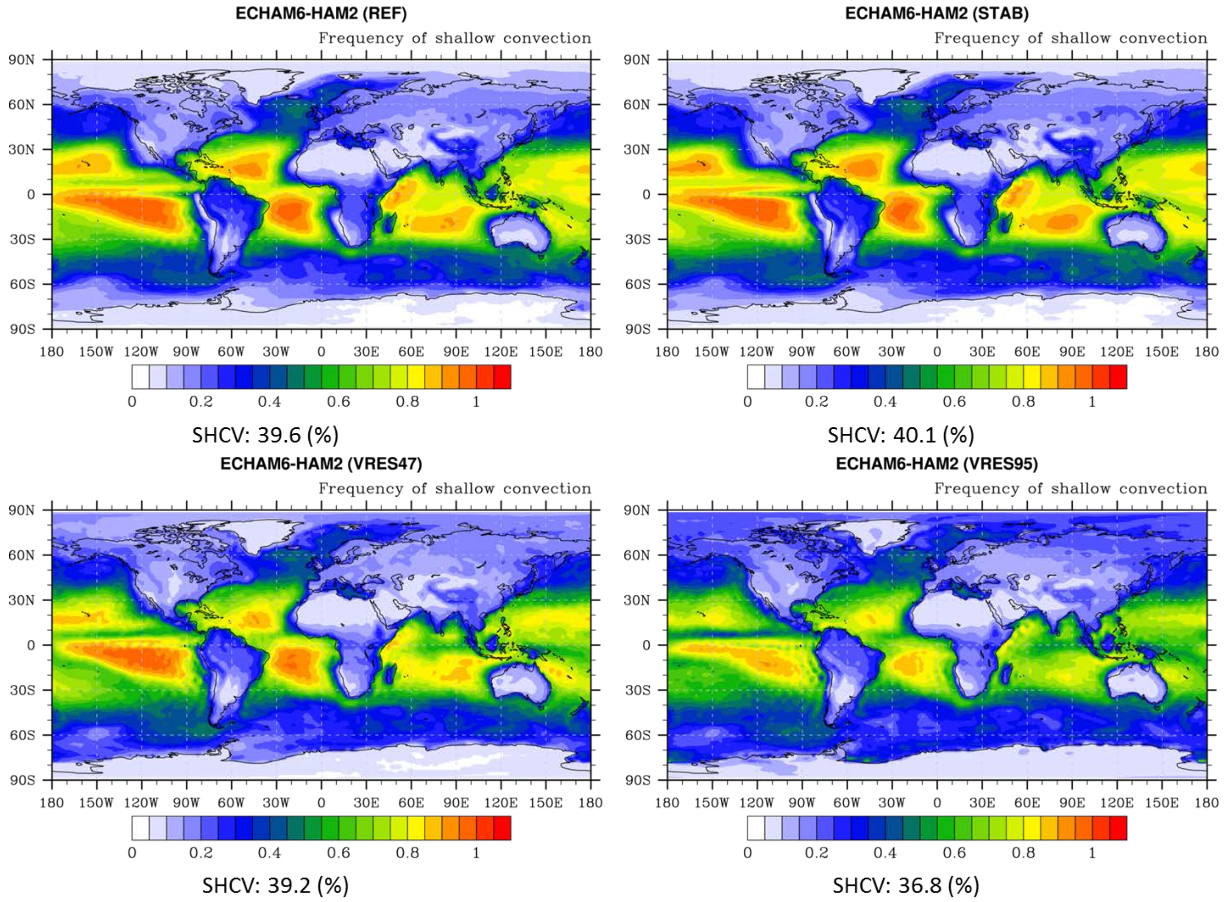

Figure C1. Frequency of the activation of the shallow-convection scheme in the REF, STAB, VRES47 and VRES95 experiments.